



## Direct observation of subtropical mode water circulation in the western North Atlantic Ocean



David M. Fratantoni\*, Young-Oh Kwon, Benjamin A. Hodges

Physical Oceanography Department, Woods Hole Oceanographic Institution, Woods Hole, MA 02543, United States

### ARTICLE INFO

Available online 26 February 2013

#### Keywords:

Atlantic Ocean  
Subtropical Circulation  
Mode Water  
Profiling Floats  
Subduction  
MBoundary Currents

### ABSTRACT

Eighteen Degree Water (EDW) is the dominant subtropical mode water of the North Atlantic subtropical gyre and is hypothesized as an interannual reservoir of anomalous heat, nutrients and CO<sub>2</sub>. Although isolated beneath the stratified upper-ocean at the end of each winter, EDW may re-emerge in subsequent years to influence mixed layer properties and consequently air–sea interaction and primary productivity. Here we report on recent quasi-Lagrangian measurements of EDW circulation and stratification in the western subtropical gyre using an array of acoustically-tracked, isotherm-following, bobbing profiling floats programmed to track and intensively sample the vertically homogenized EDW layer and directly measure velocity on the 18.5 °C isothermal surface.

The majority of the CLIVAR Mode Water Dynamics Experiment (CLIMODE) bobbers drifted within the subtropical gyre for 2.5–3.5 years, many exhibiting complex looping patterns indicative of an energetic eddy field. Bobber-derived Lagrangian integral time and length scales (3 days, 68 km) associated with motion on 18.5 °C were consistent with previous measurements in the Gulf Stream extension region and fall between previous estimates at the ocean surface and thermocline depth. Several bobbers provided evidence of long-lived submesoscale coherent vortices associated with substantial EDW thickness. While the relative importance of such vortices remains to be determined, our observations indicate that these features can have a profound effect on EDW distribution. EDW thickness (defined using a vertical temperature gradient criterion) exhibits seasonal changes in opposition to a layer bounded by the 17 °C and 19 °C isotherms. In particular, EDW thickness is generally greatest in winter (as a result of buoyancy-forced convection), while the 17°–19 °C layer is thickest in summer consistent with seasonal Ekman pumping. Contrary to previous hypotheses, the bobber data suggest that a substantial fraction of subducted EDW is isolated from the atmosphere for periods of less than 24 months. Seasonal-to-biennial re-emergence (principally within the recirculation region south of the Gulf Stream) appears to be a common scenario which should be considered when assessing the climatic and biogeochemical consequences of EDW.

© 2013 Elsevier Ltd. All rights reserved.

### 1. Introduction

Eighteen Degree Water (EDW) is the archetype for the anomalously thick and vertically homogenous mode waters typical of all subtropical western boundary current systems (e.g. Hanawa and Talley, 2001). EDW, the subtropical mode water of the northwestern Atlantic Ocean (e.g. Worthington, 1959), is notable for both its vertical homogeneity (a minimally-stratified layer 200–500 m thick; Fig. 1) and horizontal extent (~40° in longitude and ~20° in latitude). EDW is in direct contact with the atmosphere only during wintertime and only in limited areas within the Gulf Stream and an adjacent recirculation to the south

(Alfultis and Cornillon, 2001; Joyce, 2012, Joyce et al., 2013 Kwon, 2003; Talley and Raymer, 1982). Elsewhere, and for the remainder of the year, EDW is isolated from direct contact with the atmosphere by the stratified upper ocean.

Observational analyses (e.g. Kwon and Riser, 2004) and numerical modeling studies (e.g. Forget et al., 2011; Old and Haines, 2006) have shown that the large volume of EDW formed each winter and isolated below the seasonal thermocline has the potential to store and integrate (i.e. “remember”) the consequences of air–sea exchange for several years. As a result, EDW impacts climate and marine ecosystems by serving as an inter-annual reservoir of anomalous heat, nutrients and CO<sub>2</sub> (Bates et al., 2002; Dong and Kelly, 2004; Dong et al., 2007; Kwon and Riser, 2004; Palter et al., 2005). A notable characteristic of EDW is that its volume is anti-correlated with the total upper ocean heat content in the subtropical gyre, so that EDW is actually a deficit

\* Corresponding author. Tel.: +1 508 289 2908; fax: +1 508 457 2181.  
E-mail address: [dfratantoni@whoi.edu](mailto:dfratantoni@whoi.edu) (D.M. Fratantoni).

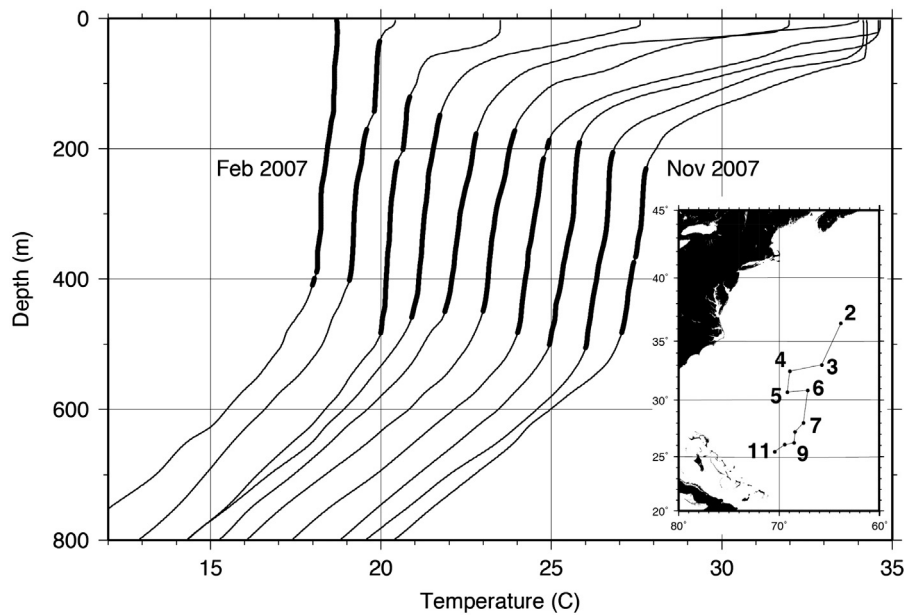


**Fig. 1.** Sequence of monthly deep (0–1000 m) temperature profiles collected by CLIVAR Mode Water Dynamics Experiment (CLIMODE) bobber 474 between February and November 2007. For clarity, all profiles are truncated at 800 m depth and profiles subsequent to the first are shifted by +1 °C relative to the preceding profile. The highlighted segments of each profile meet the temperature and temperature gradient criteria for Eighteen Degree Water (EDW) as proposed by Kwon and Riser (2004) and discussed in Appendix A. During this 10-month period the bobber drifted southward from approximately 38°N to 28°N. Profile positions are labeled by month number in the inset.

heat reservoir (Dong et al., 2007; Kwon, 2003). That is, winters with greater air–sea cooling result in a thicker and slightly cooler variant of EDW, and vice versa (Kwon and Riser, 2004; Talley and Raymer, 1982).

EDW, formed near the surface during a period of high primary productivity (Siegel et al., 2002), is nutrient-poor. A recent analysis of historical hydrographic data (Palter et al., 2005) has suggested that EDW formation and advection can influence biogeochemical processes in the subtropical gyre by introducing variability in the subsurface nutrient reservoir. In particular, Palter et al. (2005) suggest that both spatial and interannual changes in EDW formation may have consequences for subsequent productivity hypothesized to be limited by nutrient delivery from below the euphotic zone.

The mechanisms and consequences of EDW formation have been studied and debated for decades (e.g. Joyce, 2012; Speer and Tziperman, 1992; Thomas, 2005; Thomas and Joyce, 2010; Warren, 1972; Worthington, 1959, 1972; see Marshall et al., 2009, for a review), yet substantial questions remain regarding the rates and mechanisms of EDW formation, dispersal, and decay. In particular, little is known of the character and intensity of the circulation at the depth of the EDW layer and the role played by meso- and submesoscale phenomena unresolved by previous measurement programs. In addition, while several estimates of the EDW formation rate have been proposed in recent years (typically an annualized 5–15 Sv; e.g. Forget et al., 2011; Joyce, 2012; Joyce et al., 2013; Kwon and Riser, 2004; Speer and Tziperman, 1992), less attention has been paid to the mechanisms responsible for the required comparable rate of EDW destruction (i.e. restratification). Hypothesizing that meso- and submesoscale circulation features contribute to both the wide dispersal and eventual destruction of EDW, we designed an experiment to directly measure the character and intensity of circulation at the depth of the EDW thermostad with appropriate temporal and spatial resolution.

The 2005–2007 CLIVAR Mode Water Dynamics Experiment (CLIMODE) field campaign (Marshall et al., 2009; see <http://climode.org>) resulted in a unique and comprehensive array of

EDW-related measurements including air–sea fluxes, detailed hydrographic and velocity observations within the Gulf Stream, and gyre-scale measurements of upper-ocean circulation and stratification. The program incorporated five research cruises conducted between November 2005 and November 2007, including two extensive mid-winter cruises in the Gulf Stream. As one component of this effort, 40 acoustically-tracked, bobbing, profiling floats (“bobbies”) were used to explore, in a Lagrangian sense, the processes responsible for the dispersal and eventual destruction of EDW in the western North Atlantic subtropical gyre. In this contribution we describe the bobber measurement program and present unique measurements of the northwestern Atlantic circulation at the depth of the EDW thermostad during the CLIMODE observational period.

The remainder of this paper is structured as follows: In Section 2 we describe our instrumentation and sampling methods. Examples of the fundamental trajectory and stratification measurements collected by the CLIMODE bobber array are presented in Section 3. In Section 4 we synthesize these measurements into basin-scale composites to infer general patterns of EDW circulation in the northwest Atlantic. Finally, in Section 5 we provide a brief summary of our findings and suggest avenues for further study.

## 2. Methods

During the 1991–1993 Subduction Experiment in the eastern North Atlantic, acoustically-tracked SOFAR floats (Rossby et al., 1975) were deployed with active buoyancy control to track the motion and evolution of a subducting slab of water (James Price, personal communication; see Joyce et al., 1998). The CLIMODE bobbies were initially inspired by this earlier work of Price. Rossby and Prater (2005) subsequently used isopycnal RAFOS floats equipped with modest buoyancy control to explore changes in layer thicknesses along Lagrangian trajectories in the North Atlantic Current.

The CLIMODE bobbies are modified APEX (Autonomous Profiling Explorer; Teledyne Webb Research Corp., E. Falmouth, MA)

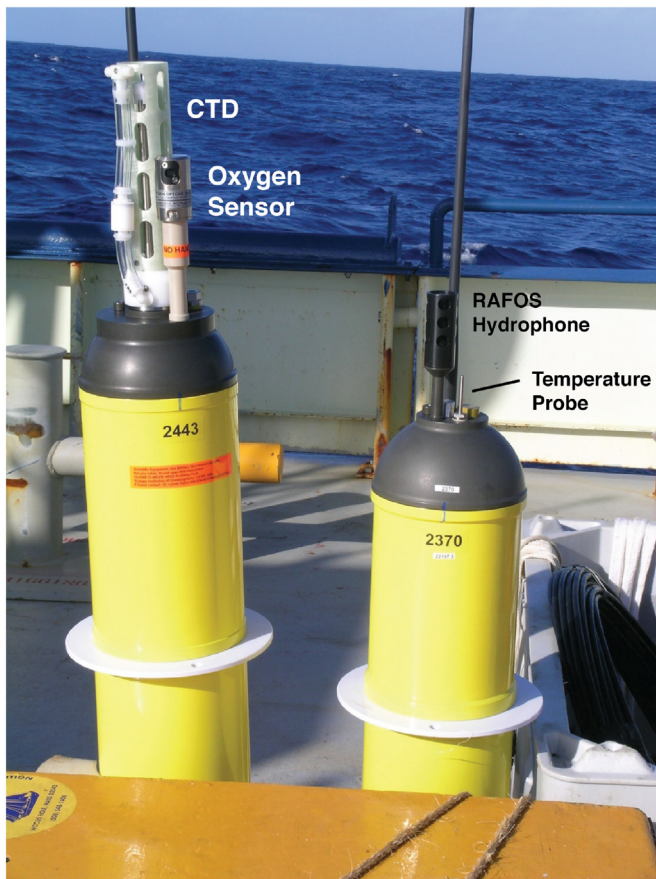


**Fig. 2.** Visual comparison of (left) a conventional Argo float equipped with conductivity–temperature–depth (CTD) and dissolved oxygen sensors, and (right) a CLIVAR Mode Water Dynamics Experiment (CLIMODE) bobber with temperature sensor and a RAFOS hydrophone. The Argo float is larger, heavier, and designed for deep isobaric operation over a long time period. The CLIMODE bobber hardware and software is optimized for actively-ballasted isothermal drift and rapid profiling at relatively shallow depths.

profiling floats comparable in form and function to those comprising the current global Argo array (e.g. Davis et al., 1992, 2001; Roemmich et al., 2009). Briefly, a profiling float is a 1.5 m, 25 kg, satellite-tracked quasi-Lagrangian drifter which periodically descends and ascends vertically through the ocean by changing its effective density (ratio of mass to volume, i.e. buoyancy) relative to that of the surrounding water. In practice, this is done by altering the volume of the float: Fluid (generally oil) is moved via pump or piston between a reservoir within an aluminum pressure hull and a flexible external bladder. The (constant) total mass of a bobber is set in the laboratory based on anticipated oceanic temperature and density conditions. For a float correctly ballasted for its region of operation a volume change of 200 cm<sup>3</sup> results in an ascent/descent rate of approximately 10 cm/s.

The differences between an “Argo float” and a “CLIMODE bobber” are few but significant. Several of these differences are visually apparent (Fig. 2) while others are software-based and evident only in the behavior of the deployed instrument. EDW generally occupies only the upper few hundred meters of the water column. Thus floats intended to remain within the EDW layer must be capable of achieving and maintaining neutral buoyancy at depths much shallower than the 1000 m parking depth typical of Argo floats, including within the minimally-stratified and turbulent wintertime mixed layer. To this end the CLIMODE bobber’s aluminum pressure hull was designed to be shorter, thinner, and lighter than typical and substantially greater onboard energy (in the form of primary lithium batteries) was allocated to active buoyancy control.

Unlike the standard conductivity–temperature–depth (CTD) instrument carried by Argo floats (e.g. Roemmich et al., 2009) the bobbers were equipped with temperature and pressure sensors only. In the western North Atlantic the relationship between temperature and salinity near the EDW thermostad is fairly robust (Fig. 3) allowing density to be reasonably approximated from temperature alone. While others have noted interesting and relevant regional variation in salinity along density surfaces in this area (e.g. Joyce et al., 2013), a conscious decision was made to neglect direct measurement of salinity in favor of constructing and deploying a larger total number of bobbers.

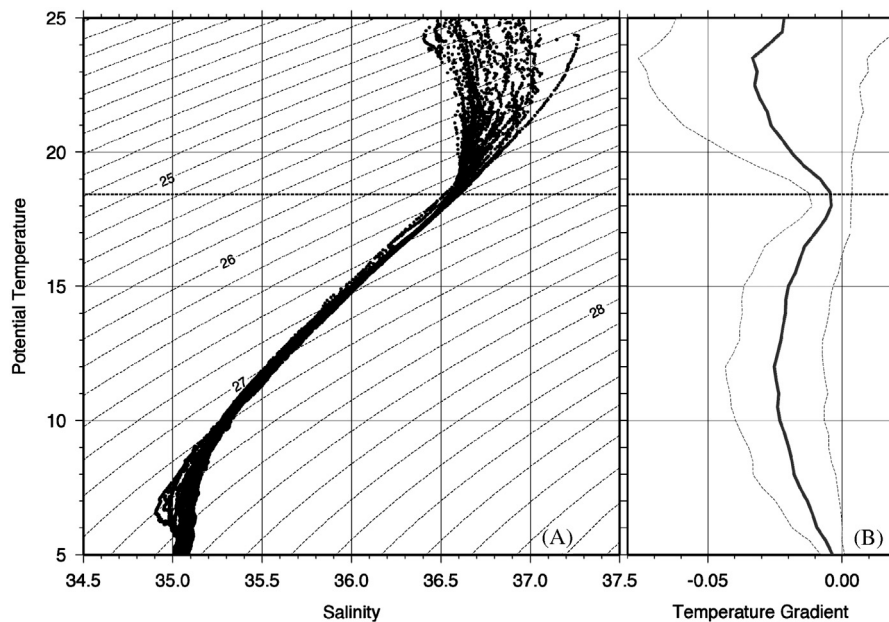


**Fig. 3.** (a) Temperature–salinity diagram illustrating the approximately linear temperature–salinity ( $T$ - $S$ ) relationship near the 18.5 °C center of the Eighteen Degree Water (EDW) layer (dotted line). Data source: stations 37–69 of 1997 WOCE A22 section in the western subtropical gyre, spanning roughly 20–40°N. (b) Representation of the mean vertical temperature gradient (°C/m) from the western subtropical gyre illustrating the local stratification minimum near 18.5 °C associated with EDW. The shaded region encompasses one standard deviation from the mean at each depth illustrating the relative spatial/temporal stability of the EDW stratification minimum. Data source: all available NODC conductivity–temperature–depth (CTD) temperature profile data since 1980 within the domain 30–38°N, 50–65°W.

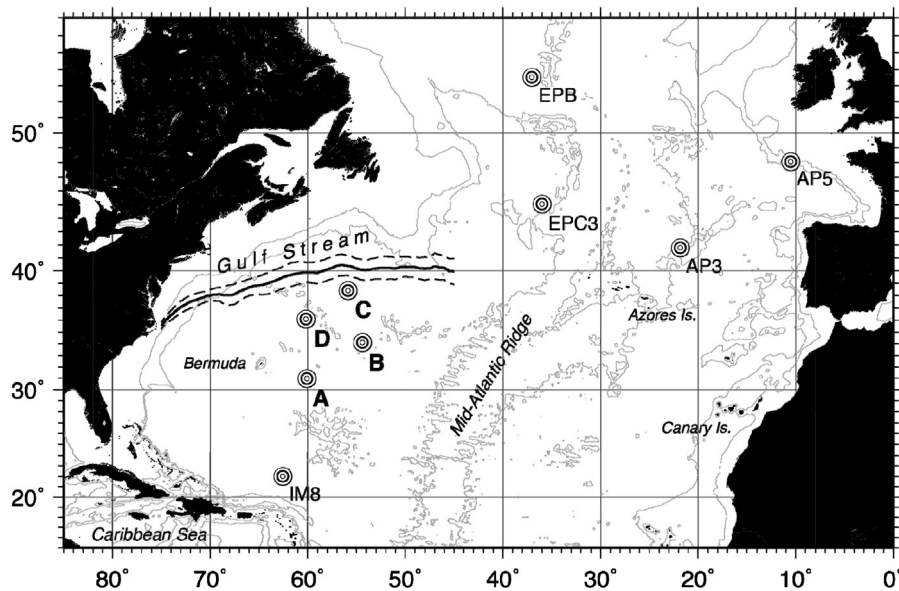


**Fig. 4.** Location of RAFOS sound source moorings used for tracking the CLIVAR Mode Water Dynamics Experiment (CLIMODE) bobbers. Source moorings A–D were deployed as part of the CLIMODE field campaign and were active between November 2005 and November 2007. Also shown are additional sound sources, active during the CLIMODE experiment, installed by investigators from the U.S. (EPB, EPC3), France (AP3, AP5), and Germany (IM8). These sources were occasionally heard by the bobbers and were used during post-experiment tracking when appropriate. In this and subsequent figures the nominal location of the Gulf Stream north wall (and a one-standard-deviation uncertainty band) is shown based on monthly-mean observations since 1966 (courtesy Fisheries and Oceans Canada/MEDS).

In addition to temperature and pressure sensors, the bobbers also carried an external low-frequency hydrophone and an internal RAFOS navigation system (Rossby et al., 1986; Seascan, Inc., Falmouth, MA) which detected daily acoustic transmissions from an array of moored sound sources. Arrival times of these transmissions were used post-experiment to determine each bobber's daily geographic position. Position records were subsequently differentiated in time to compute daily average horizontal (isothermal) bobber velocities.

The goal of this program was to directly measure the dispersal of EDW as deep wintertime mixed layers are subducted beneath the subtropical gyre stratification and/or capped by the seasonal thermocline. The bobber mission was thus designed to maximize the number of temperature and acoustically-derived position/velocity measurements within the EDW layer, with only occasional measurements above and below this layer. While Argo floats typically drift isobarically at 1000 dbar for 10 days between surfacings, the 40 CLIMODE bobbers were programmed to actively track the 18.5 °C temperature surface. Analysis of previous measurements in the region suggested that this isotherm was, with some interannual variation, grossly representative of the vertical center of the minimally-stratified EDW layer in the western Atlantic (Fig. 3). The bobber's onboard controller was programmed with a feedback loop that, informed by hourly-measured in situ temperature, adjusted the float's buoyancy by controlling the amount of oil pumped into the external bladder. The bobbers were programmed to closely ( $\pm 0.1$  °C) follow the 18.5 °C isotherm continually for 3 days, then "bob" quickly between the 17 °C and 20 °C isotherms before returning again to 18.5 °C. Bobs were completed as rapidly as possible (using the full range of the available volume change) to maximize the time spent on the 18.5 °C isotherm and minimize contamination of the horizontal (isothermal) velocity record.

Specific behavioral rules were devised in case a bobber should fail to locate one of its target isotherms. For example, each bobber was instructed to maintain an isobaric position of 50 dbar should the 18.5 °C isotherm be unattainable (e.g. during wintertime surface exposure of the EDW layer). The alternative – drifting at

the surface – would have contaminated the position/velocity record due to the direct action of wind and surface waves on the bobber. The drift/bob cycle was repeated 10 times over 30 days, punctuated with a final descent to 1000 m before surfacing to transmit temperature, pressure, RAFOS, and engineering data via satellite. Bobbers remained on the surface for approximately 12 hours each month during CLS/Argos satellite data transmission.

The bobbers were acoustically tracked using an array of four moored sound sources (Fig. 4) built at the Graduate School of Oceanography, University of Rhode Island (T. Rossby, personal communication). Each source emitted a daily, 80 s, 260 Hz swept signal detectable for hundreds to thousands of kilometers. The source moorings were deployed in November 2005 and recovered in November 2007. Additional sound sources deployed in the North Atlantic by investigators from the US, France, and Germany were occasionally heard by the bobbers and were used during post-experiment tracking. Time-series measurements of temperature, salinity, and velocity were recorded at several depths on each source mooring. Details of the CLIMODE subsurface moored measurements are described elsewhere (e.g. Davis et al., 2013).

In summary, each bobber yielded daily-resolved position, velocity, and pressure; 3-day-resolved EDW stratification and thickness; and monthly-resolved 0–1000 m temperature profiles. Vertical resolution of temperature ranged from 5 m near the surface to 20 m below 500 m depth.

### 3. Results

#### 3.1. Bobber performance and data return

From an engineering perspective overall bobber performance was excellent: 28 of 40 bobbers had a 100% success rate (actual/expected satellite transmissions of valid data) and 38 of 40 had a success rate greater than 90%. Bobber lifetimes were substantially greater than anticipated: the half-life of the bobber array exceeded

4 years, almost twice as long than the overall duration of the CLIMODE field campaign. A timeline illustrating the lifetime of the bobber array is shown in Fig. 5.

During the CLIMODE experiment acoustic detection ranges were reduced versus more typical deep RAFOS float applications due to the shallow depth of the bobbers (well above the SOFAR channel and occasionally within the mixed layer) and the strong lateral density gradients associated with the Gulf Stream and its rings. Nevertheless, source transmissions were detected at ranges as large as 2000 km (Fig. 6). Most valid positions were determined using sources at ranges less than 1000 km. Post-experiment acoustic tracking (Wooding et al., 2005) enabled position and velocity estimation with a temporal resolution of 1 day and geographic uncertainty (relative to CLS/Argos satellite-derived surface position) of approximately 5 km (see Fratantoni et al., 2010). Errors in absolute positioning are due primarily to poorly-resolved non-constant clock drift on both sources and receivers. Thirty-seven of 40 bobbers were acoustically tracked over all or part of their lifetime. Additional details regarding bobber performance and the acoustic tracking procedure can be found in Fratantoni et al. (2010).

Bobbers were primarily deployed in winter (January 2006 and February 2007) along the southern edge of the Gulf Stream (Fig. 7). Additional bobbers were deployed during mooring deployment and turn-around cruises in November 2005 and November 2006. Care was taken to deploy bobbers south of the Gulf Stream axis to minimize the loss of instruments from the subtropical gyre to the slope water north of the Gulf Stream.

The bobbers returned two independent data types: temperature profiles and acoustically-derived position/velocity measurements. The profile data described herein include that obtained between July 2005 and May 2009. Due to the limited deployment duration of the CLIMODE sound source moorings, acoustic tracking was only available between November 2005 and November 2007. A census of available data (Fig. 8) demonstrates that the total number of monthly temperature profiles (bobs and deep profiles combined) increased with each deployment cruise until the final bobbers were launched in March 2007, and then slowly declined. The number of valid RAFOS velocity measurements likewise increased with time until the source

array was recovered in late November 2007. The distribution of temperature profiles by month is fairly consistent. Due to preferential wintertime deployments and a shorter 2-year measurement window, RAFOS velocity measurements are skewed slightly towards the spring and summer seasons.

Every third day, each bobber rapidly descended from its parking depth on the 18.5 °C isotherm to the depth of the 17 °C isotherm, ascended to the 20 °C isotherm, and then returned to the 18.5 °C isotherm. As expected, the bounding depths of these bobs varied with both season and latitude. Most bobs sampled a vertical interval from approximately 100–500 m depth (Fig. 9). The dominant modes shown in the bob top, bottom, and extent histograms approximate

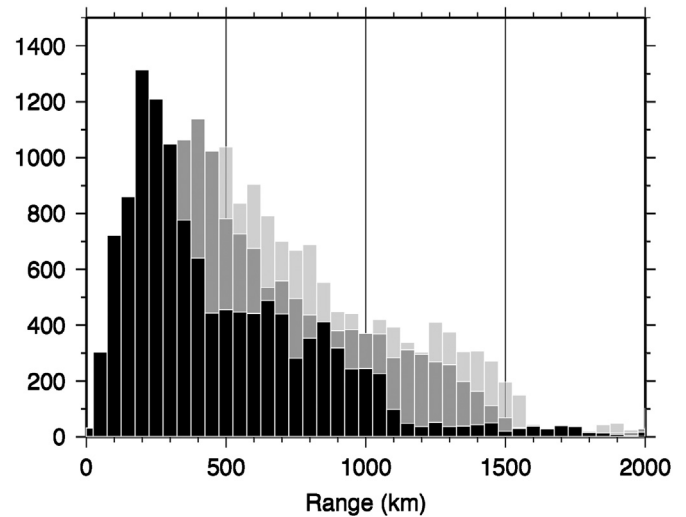


Fig. 6. A valid RAFOS position measurement requires detection of transmissions from at least two moored sound sources. Shown here is the distribution of range from each valid bobber position to the three closest sources (closest source range indicated by darkest bar) at the time of each valid position/velocity measurement. A majority of the valid RAFOS position solutions were achieved within 500 km of the closest sound source.

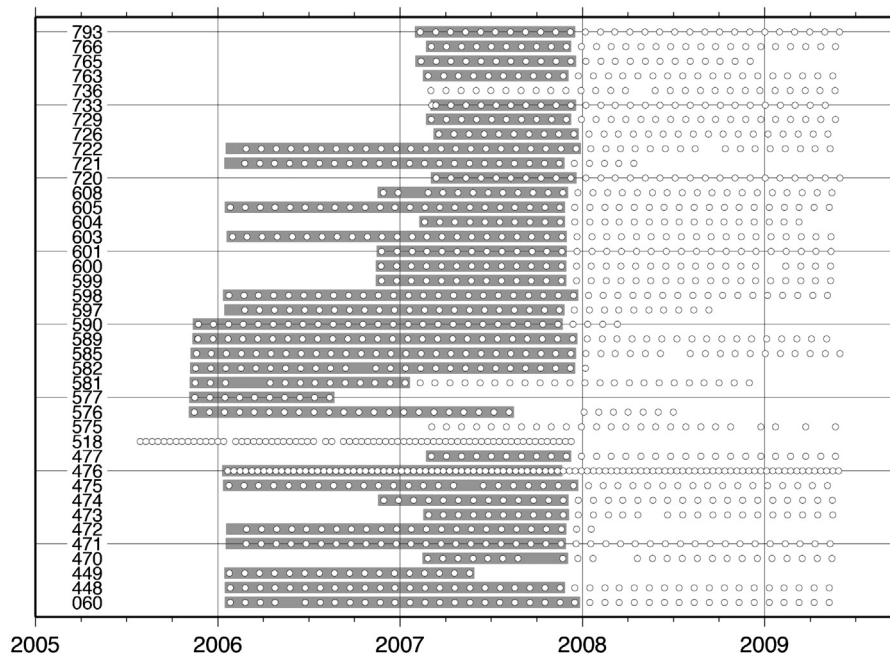


Fig. 5. Timeline illustrating the lifetime of each CLIMODE bobber. Open circles indicate receipt of an Argos-derived position report from each bobber. The shaded portions of each bobber's timeline indicates the period over which acoustic tracking was successful. For testing purposes, two bobbers (518 and 476) were instructed to surface every 12 days rather than the standard 30 days.

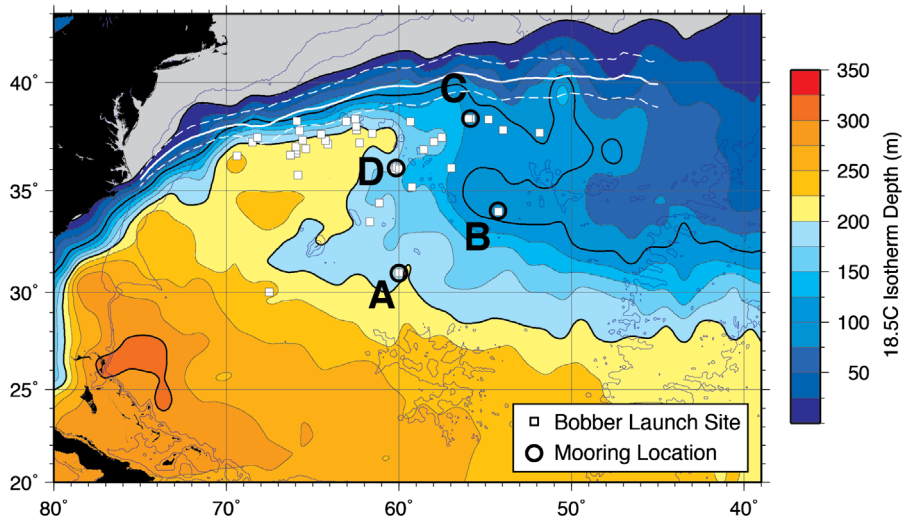


Fig. 7. Position of CLIVAR Mode Water Dynamics Experiment (CLIMODE) bobber deployments and the moored sound source array. Also shown is the annual mean depth of the 18.5 °C isotherm as derived from historical hydrographic data (Curry, 1996).

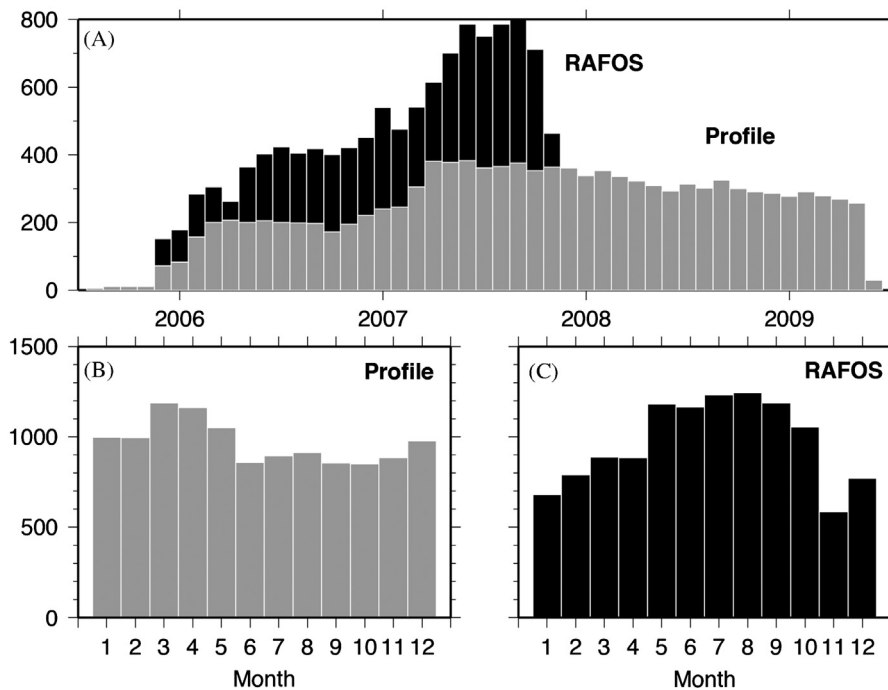


Fig. 8. Histograms of (a) the number of RAFOS and profile measurements obtained by the bobber array during each month of the CLIVAR Mode Water Dynamics Experiment (CLIMODE) field campaign, and (b and c) the average monthly distribution of these data.

the regional- and time-averaged distributions of the 17° and 19 °C isotherms and their vertical separation, respectively. Where the 20 °C isotherm did not exist the bobber was allowed to profile to the surface—values corresponding to a bob-top depth of zero have been suppressed in Fig. 9. The near-surface mode of the “bob-bottom” histogram results from situations in which neither bounding isotherm existed—a state which can only be realized after the bobber completes a finite vertical excursion to measure the stratification.

### 3.2. Bobber trajectories

Fig. 10 summarizes the trajectories of the CLIMODE bobbers. In Fig. 10a, only initial and final positions are shown to illustrate the overall displacement of the bobbers from their deployment locations. In Fig. 10b, low-resolution Argos satellite tracking

provides roughly 30-day position resolution of each bobber trajectory. The great majority of bobbers exhibited a net southward displacement and remained within the western subtropical gyre for at least 2.5–3.5 years. Several bobbers did escape the subtropics by moving northward across the Gulf Stream/ North Atlantic Current east of the Grand Banks between 30 and 40°W. The fraction of bobbers escaping the subtropical gyre (three of 40) is comparable to that found by Kwon and Riser (2005), seven of 71, and also similar to surface drifter studies by Brambilla and Talley (2006) and Rypina et al. (2011).

The most adventurous bobber drifted through the eastern Norwegian Sea and was last heard from the Arctic Ocean at 79°N near Spitsbergen. A single bobber passed southward into the Caribbean Sea through the Anegada Passage east of Puerto Rico and nearly reached the Yucatan Strait. Although most bobbers

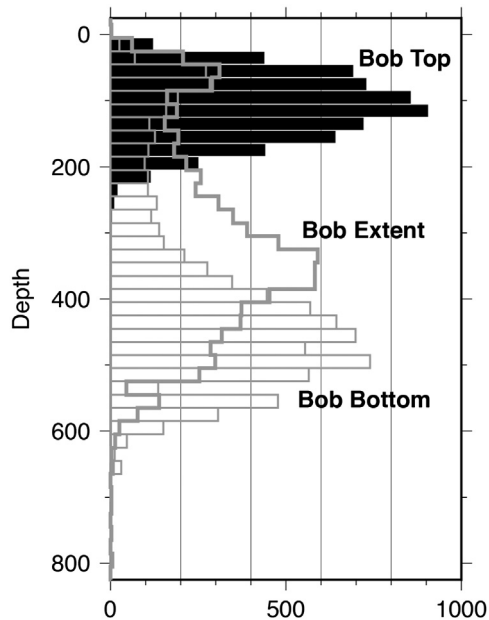


**Fig. 9.** Histograms of the depth of the top (shallow limit), bottom (deep limit), and total vertical extent of each 17–20 °C bob performed by the bobber array. Where the 20 °C isotherm did not exist the bobber was allowed to profile to the surface—values corresponding to a depth of zero have been suppressed in this figure.

were contained within the western subtropical gyre, eight eventually drifted eastward across the mid-Atlantic ridge with two reaching the Canary Basin.

As described above, the bobbers collected both position/velocity measurements (daily) and temperature profiles (every third day). Fig. 11 summarizes the geographic distribution of these measurements in a smaller region of the western subtropical gyre within which our analyses will focus. Fig. 11a illustrates the spatial distribution of stratification measurements including both every third day EDW-centric bobs (blue) and monthly 1000 m deep profiles (red). Profile locations are presented using the best-available positioning method: acoustic RAFOS tracking if available, and linearly-interpolated Argos satellite tracking otherwise. As per the experiment design, measurement density is greatest to the south of the Gulf Stream and diminishes rapidly east of 45°W (the mid-Atlantic ridge) and south of 30°N.

Fig. 11b presents a composite of all valid acoustically-tracked bobber trajectory segments. This figure provides an unprecedented overview of the general character of circulation on a temperature surface associated with the vertical center of the EDW layer. Immediately notable in Fig. 11b are loops and swirls associated with bobbers trapped within various recirculations, eddies, and (in a few cases) long-lived, translating, coherent vortices. Several of these features will be examined in greater detail below.

Trajectory information near the Gulf Stream and mid-Atlantic Ridge is occasionally fragmented due to the difficulties encountered in post-experiment acoustic tracking. Throughout this contribution only trajectory information collected from bobbers drifting on the appropriate temperature surface ( $18.5\text{ °C} \pm 0.1\text{ °C}$ ) will be used for display and analysis. In order to most effectively describe the trajectory of each bobber over its complete lifetime, we use composite best-available trajectories consisting of high-resolution RAFOS-tracked position data supplemented by Argos satellite tracking when required. A sample of 16 such composite trajectories illustrating the substantial variation in regional circulation patterns is shown in Fig. 12 (cf. Kwon and Riser, 2005).

The Gulf Stream's zonal extension defines the northern extent of the subtropical gyre and is the dominant circulation feature in

the northwest Atlantic. Several bobbers deployed just south of the Gulf Stream were swept rapidly eastward (with speeds exceeding 70 cm/s) to 50–60° W before slowly drifting into the gyre interior (e.g. bobbers 448, 721, and 766 in Fig. 12). Bobbers deployed slightly further south within the moored array (e.g. 577, 585, 604 in Fig. 12) did not encounter the eastward Gulf Stream and drifted generally southward and/or westward. A total of 13 of 40 bobbers drifted sufficiently south and west to re-enter the northward western boundary current flow (Antilles Current, Florida Current, or Gulf Stream depending on latitude) and recirculate within the subtropical gyre. Six examples of this behavior are shown in Fig. 12 (e.g. 474, 518, 585). A large fraction of the trajectories shown in Fig. 12 demonstrate substantial southward movement between 50 and 60°W, consistent with altimeter-derived mean dynamic topography (e.g. Jayne, 2006; see below Fig. 17).

### 3.3. Case studies: stratification and along-track EDW thickness evolution

Four interesting examples of combined trajectory and stratification measurements are shown in Fig. 13a and b. In addition to the observed quantities of position, temperature and pressure, these figures also illustrate the derived RAFOS velocities and the time variation of EDW thickness (see Appendix A) computed along the bobber trajectory.

#### 3.3.1. Bobber 448: long trajectory, minimal EDW thickness

This bobber (Fig. 13A) experienced three full annual cycles during its lifetime but only tracked a significant amount of EDW during the first 3 months of its mission. Deployed just south of the Gulf Stream in January 2006, this bobber was swept eastward for several days before drifting south into the gyre interior near 50°W. Initially drifting isothermally at 300 m on 18.5 °C, the bobber rose to within 50 m of the surface while in the Gulf Stream before moving rapidly southward beneath the warmer surface waters of the subtropical gyre. Upon deployment the local EDW thickness was approximately 150 m. This increased to 400 m in the wintertime Gulf Stream but decayed to near zero as the bobber moved southward to 30°N over the next 3 months. By July 2006 the bobber was south of 30°N on the western flank of the mid-Atlantic Ridge and the local EDW thickness had vanished completely. Note that the thickness of the 17–19 °C layer alone (gray curve in panel (d)) does not adequately capture the evolution of EDW thickness—the temperature gradient criterion (Appendix A) allows us to discriminate the minimally-stratified mode water from the background stratification. This distinction is important, as potential vorticity conservation (for example,  $f/H$  where  $f$  is the Coriolis parameter and  $H$  the local layer thickness—an approximation valid for low-Rossby number, large-scale circulation) implies that the 17–19 °C layer must thin to compensate for the reduction in planetary vorticity as the water parcel (i.e. the bobber) is advected equatorward.

#### 3.3.2. Bobber 721: minimal translation, annual re-emergence

Though deployed at almost the same time and position as the previous example, bobber 721 (Fig. 13A) remained north of 32°N for most of its lifetime and tracked a substantial layer of EDW through two annual cycles. EDW thickness increased from 200 m to 450 m during the first winter, then remained steady at 150–200 m. The bobber was re-exposed to the mixed layer along the southern edge of the Gulf Stream in March–April 2007 resulting in a second transient thickness increase. EDW thickness decreased (and bobber depth increased) as it migrated southwestward towards Bermuda in September 2007.

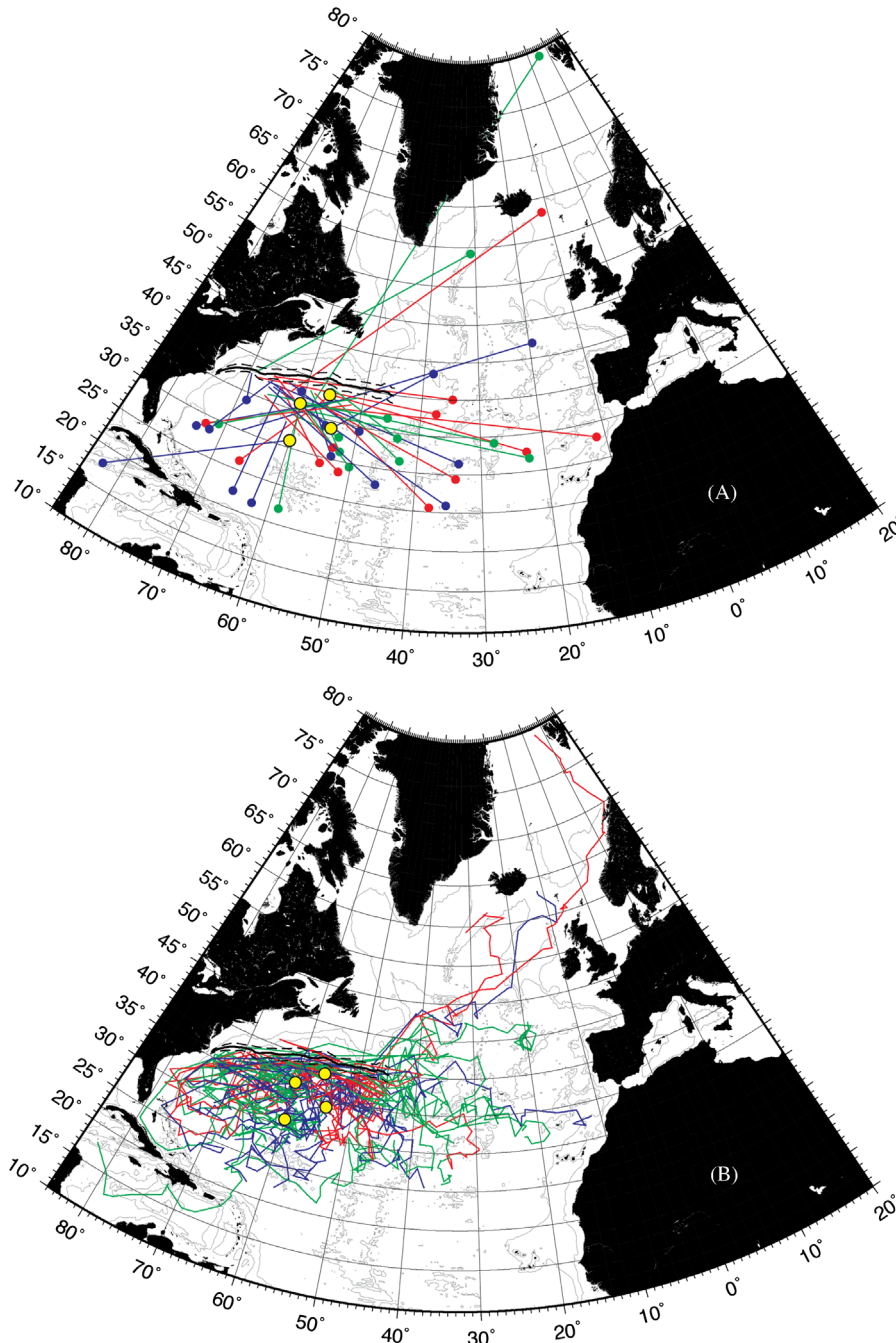


**Fig. 10.** (a) Total lifetime displacement of each CLIVAR Mode Water Dynamics Experiment (CLIMODE) bobber from its launch location. Final position is indicated with a filled circle. The sound source array is indicated by the yellow circles. (b) Argos-derived trajectories showing the drift of each bobber at approximately 30-day temporal resolution. In both panels the colors assigned to trajectories are random and arbitrary.

### 3.3.3. Bobber 598: gradual EDW decay, western boundary encounter

Also deployed south of the Gulf Stream in January 2006, bobber 598 (Fig. 13B) illustrates several scenarios observed frequently during this experiment: (a) extended and vigorous recirculation between 35°N and the Gulf Stream, (b) southwestward translation including a variety of looping behaviors characteristic of mesoscale eddies accompanied by gradual reduction in local EDW thickness, and (c) an encounter with the western boundary and re-absorption into the Gulf Stream system. An initial EDW thickness of 200 m decayed to less than 50 m over 8 months (November 2007–August 2008) as the bobber moved southwestward from the recirculation region towards the Bahamas. Although poorly resolved by monthly

Argos-only tracking after November 2007, it is evident that the bobber re-entered the western boundary current and eventually crossed to the north side of the Gulf Stream where the surface temperature was substantially lower.

### 3.3.4. Bobber 474: long-lived anticyclonic eddy, western boundary encounter

As a final example, bobber 474 (Fig. 13B) was deployed in November 2006 at 300 m depth in a 200 m thick EDW layer near the southern edge of the Gulf Stream. Following deployment the bobber moved southwestward while occasionally looping with no

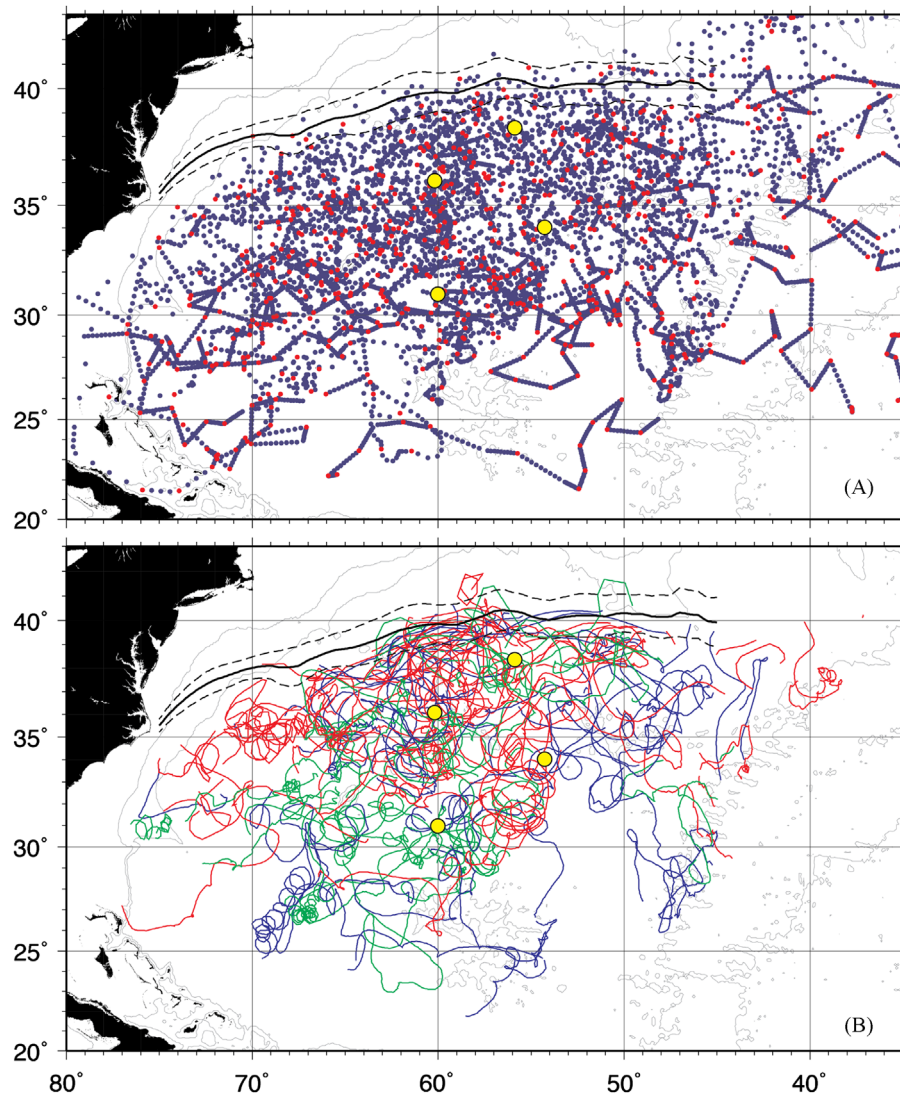


**Fig. 11.** (a) Position of each valid bob profile (blue dot) and deep (1000 m) profile (red dot) reported by the bobber array. (b) Final record-length RAFOS-derived isothermal (18.5 °C) trajectories and fragments for all trackable bobbers. Discontinuities in several trajectories are due to intermittent periods in which range, topography, or stratification issues resulted in inability to compute accurate position estimates, or in which the bobber deviated from the target 18.5 °C parking isotherm. The colors assigned to trajectories are random and arbitrary.

preferred sense of rotation. The local EDW thickness remained near 300 m for almost a year following a brief wintertime thickening to nearly 500 m. In late summer of 2007 this bobber began looping anticyclonically and remained trapped within a long-lived translating eddy for more than 4 months. A more detailed view of the looping portion of this trajectory is shown in Fig. 14. Subsequent investigation of this and similar features in the context of satellite altimetry and co-located surface drifters (Park et al., 2012) suggests a strong correlation between surface vortices and those revealed by the bobbers at EDW depth.

#### 4. Basin-scale synthesis

To investigate low-frequency, basin-scale aspects of EDW circulation the bobber measurements were averaged in spatial bins to construct quasi-Eulerian fields of velocity, eddy kinetic energy (EKE), isotherm depth, and EDW thickness. Although the bobber measurements cover only a fraction of the North Atlantic, they do provide a unique and high-resolution snapshot of EDW structure and circulation during the CLIMODE field experiment.

Additional contemporary measurements including ongoing Argo profiling float observations provide a broader spatial and temporal context for the bobbers, and are examined in separate contributions (e.g. Park et al., 2012) and in future work.

##### 4.1. Velocity statistics and mean fields

The fields presented below are based on observations grouped into  $2^\circ \times 2^\circ$  boxes. In any such analysis there is a trade-off between spatial resolution, areal coverage, and statistical reliability of the box-averaged quantities. This box size was chosen subjectively to provide a reasonable depiction of the circulation while ensuring that most boxes contain sufficient data to form statistically reliable mean values. To that end, 90-day non-overlapping segments of isothermal bobber velocity were used to estimate the Lagrangian time and length scales associated with EDW circulation in the western North Atlantic (see e.g. Lumpkin et al., 2002). The valid isothermal velocity observations were distributed vertically with a mean depth of 185 m and standard deviation of 80 m. The velocity autocorrelation function (Davis, 1991; see Lumpkin et al., 2002 for the specific definition used herein) was computed for each of 75 such segments,

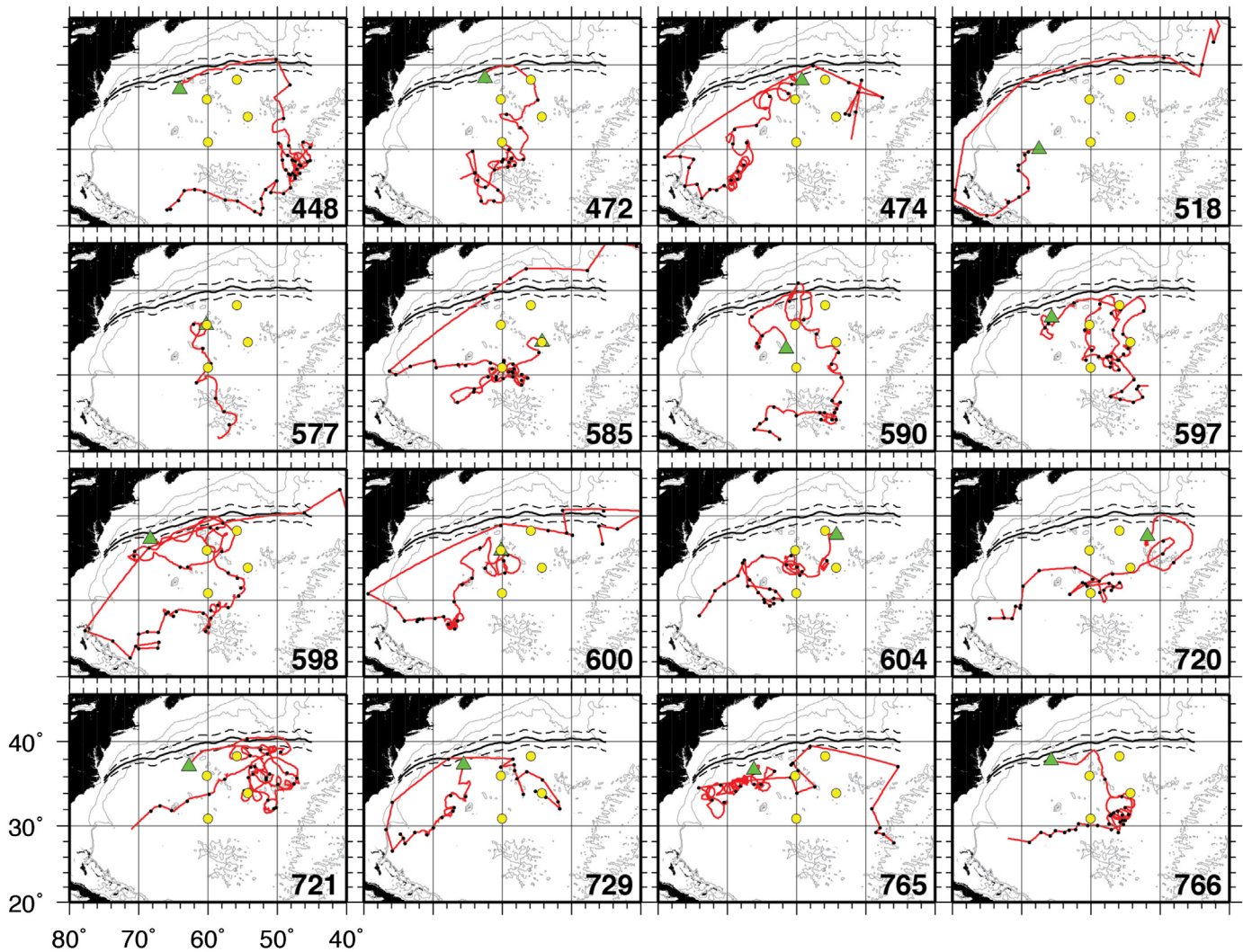


**Fig. 12.** Composite (RAFOS+Argos) trajectories of 16 CLIVAR Mode Water Dynamics Experiment (CLIMODE) bobbers on the 18.5 °C temperature surface in the western North Atlantic subtropical gyre. Bobber deployment location is indicated by a green triangle in each panel. Small black dots are shown at 30-day intervals along each trajectory.

then ensemble averaged and integrated to the first zero crossing to yield a Lagrangian integral timescale estimate ( $T_L$ ; see Lumpkin et al., 2002) of approximately 3.2 days. No significant differences were noted between  $T_L$  computations using meridional vs. zonal components of velocity. The Lagrangian integral length scale ( $L_L$ ) is related to  $T_L$  via a characteristic speed,  $L_L = u' T_L$ . Taking  $u'$  as the RMS velocity magnitude averaged over the seventy-five 90-day trajectory segments (approximately 22 cm/s) yields a length scale of approximately 68 km, or roughly twice the local first-baroclinic deformation radius (30–40 km over much of the study area as reported by Chelton et al., 1998).

A sensitivity study was conducted to determine the potential impact of different segment lengths on these calculations. Segment lengths varying from 30 to 120 days resulted in time and length scales which differed by less than 7%. Based on the observed ability of monthly-surfacing bobbers to track translating features (e.g. bobber 474; Fig. 14) we are confident that monthly bobber surfacing (resulting in removal and reinsertion of the bobber from a tracked water parcel) does not significantly affect these calculations.

The estimated time, length, and velocity scales within the EDW layer are consistent with previous float and drifter measurements in the same general region as summarized by Lumpkin et al. (2002) (Fig. 15). The bobber scale estimates fall between

prior measurements at the surface and 700 m depth. In their analysis, Lumpkin et al. (2002) defined adjacent geographical regions encompassing the Gulf Stream extension and the MODE region (e.g. Rossby et al., 1983) in the southwest subtropical gyre. The bobber-derived integral scales are most similar to previous measurements in the Gulf Stream extension region. Note that there are fewer bobber measurements in the less energetic MODE region than in the vicinity of the Gulf Stream, and thus that the aggregate scale estimates reported here are biased towards the latter region. Further analysis, not included herein, is required to determine the degree of spatial and/or temporal variability in these parameter estimates.

The integral time and length scales were used to quantify the independence (i.e. the number of degrees of freedom (DOF)) of individual observations contributing to spatially-binned velocity and temperature fields. The DOF associated with each grid cell was computed by following individual bobbers as they translated through a  $2^\circ \times 2^\circ$  rectilinear grid. Measurements obtained in a given cell were judged to be independent if (a) they resulted from different bobbers, or (b) they resulted from the same bobber but that bobber remained in the box for more than one Lagrangian integral timescale (taken to be 3 days). The raw distribution of all RAFOS-derived velocity measurements and the resulting DOF

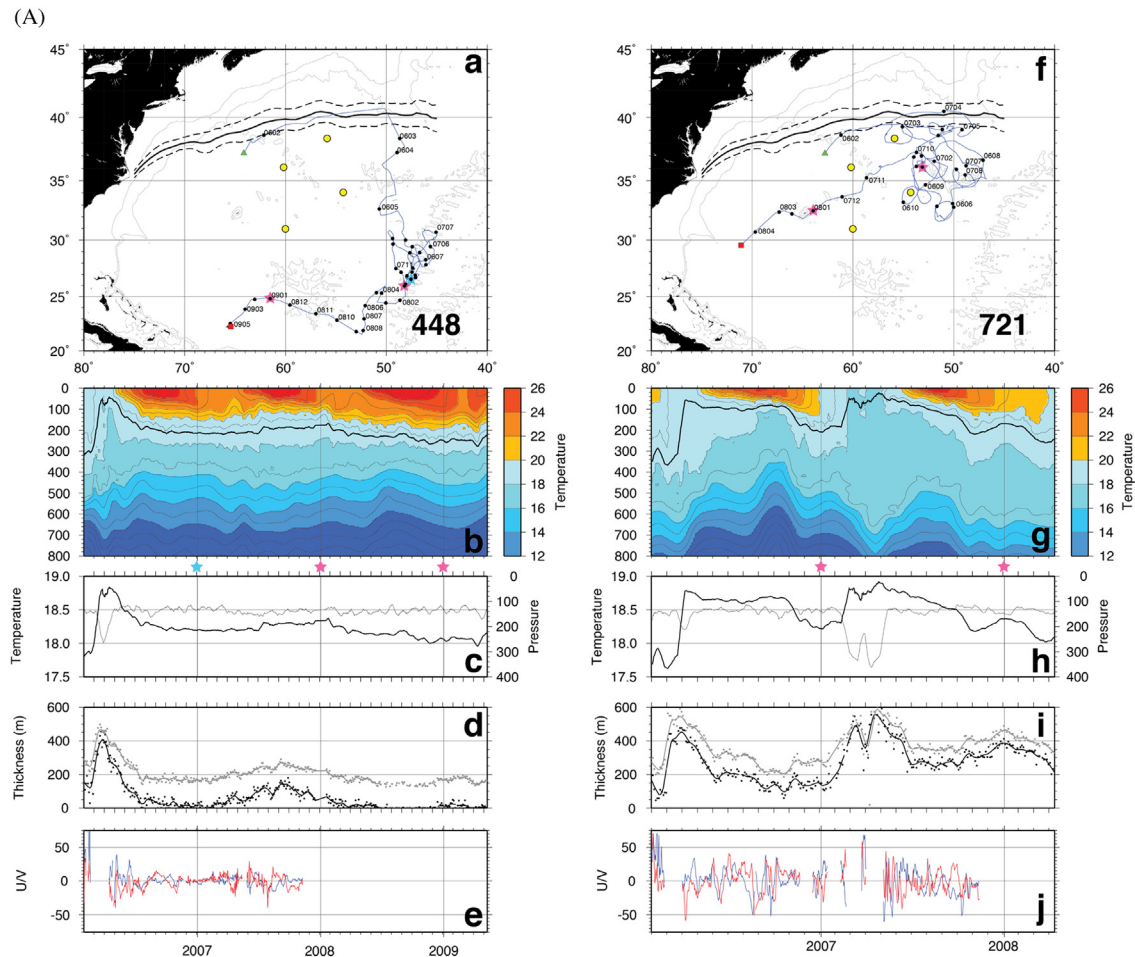


**Fig. 13.** (A) Composite trajectory, temperature stratification, drift temperature and pressure, Eighteen Degree Water (EDW) and 17–19 °C thickness, and velocity as measured by CLIVAR Mode Water Dynamics Experiment (CLIMODE) bobbers 448 (left; a–e) and 721 (right; f–j). (a) Composite (RAFOS+Argos) trajectory with monthly tickmarks and date (YYMM) labels. Initial/final bobber position indicated by the green/red triangle. (b) Temperature as a function of time and depth. Contour interval is 1 °C. The dark solid line indicates the actual drift depth of the bobber. Temporal resolution at depths between 17 and 19 °C is 3 days; below that it is 30 days. (c) Daily measured bobber temperature (light line) and pressure (dark line). The target drift temperature was 18.5 °C ± 0.1 °C. (d) Thickness (see Appendix A) of water identified as EDW using the Kwon and Riser (2004) temperature/temperature gradient criteria. Black line shown is a 30-day smoothed representation of the individual 3-day estimates (dots). Gray line and dots are corresponding estimates of 17–19 °C layer thickness. (e) Meridional (red) and zonal (blue) velocity (cm/s) computed from the RAFOS-tracked segments of the bobber trajectory. Stars highlight instrument positions on 1 January of each year. (B) As in Fig. 13a, but for bobbers 598 (left) and 474 (right).

distribution for valid, isothermal velocity measurements are shown in Fig. 16. Data density, and thus DOF, in a given area is a function of both the initial deployment strategy and the intensity of the regional circulation. For the record-length mean fields shown below, binned values obtained in regions with less than 10 DOF are ignored.

The record-length mean velocity field on the 18.5 °C isotherm is shown in Fig. 17. Note that this field does not represent the circulation of EDW specifically (the abundance and distribution of which will be described below) but rather identifies the broad patterns of circulation on an isothermal surface coincident with the expected vertical center of EDW. For comparison, we also show in Fig. 17 the mean dynamic topography of the ocean surface derived from satellite altimetry (Jayne, 2006).

At the northern extent of the domain the eastward flow of the Gulf Stream extension is readily apparent with mean values exceeding 15 cm/s. Over the remainder of the sampled domain the flow is generally southwest at speeds of 5–10 cm/s. Between 50° and 55°W the flow turns cyclonically from weak westward flow to strong (6–8 cm/s) southward flow over a short distance. A comparison of this velocity field with the climatological mean 18.5 °C isotherm depth (Fig. 7; see also Fig. 20a) indicates that this

direction change is generally coincident with the location of a strong gradient in isotherm depth near 58°W.

The densely sampled region in the center of Fig. 17, east of Bermuda near 32°N, 60°W, is interesting for its lack of significant flow. Though perhaps overemphasized in our coarse 2° × 2° presentation, it appears that modest southwestward flow bifurcates into two branches near 34°N, 57°W, leaving an apparent void over the Bermuda Rise east of Bermuda. A closer examination of non-significant mean velocities in this area (i.e. those grid cells with magnitude smaller than their standard deviation) indicates flow is generally southwestward in this region, but at a slower mean rate and with enhanced variability. The Bermuda Rise is well-known among paleoceanographers for its high sedimentation rate, believed to be caused by recirculating bottom currents associated with the westward Gulf Stream return flow (e.g. Laine and Hollister, 1981; Lund and Keigwin, 1994). The bobber observations appear to support the notion of a regionally-distinct circulation character over the Bermuda Rise, and are coincident with a relative “flat spot” in the mean dynamic topography contours suggestive of reduced mean flow.

The EKE distribution associated with the 2° × 2° averaged velocities is shown in Fig. 18 and compared with previously

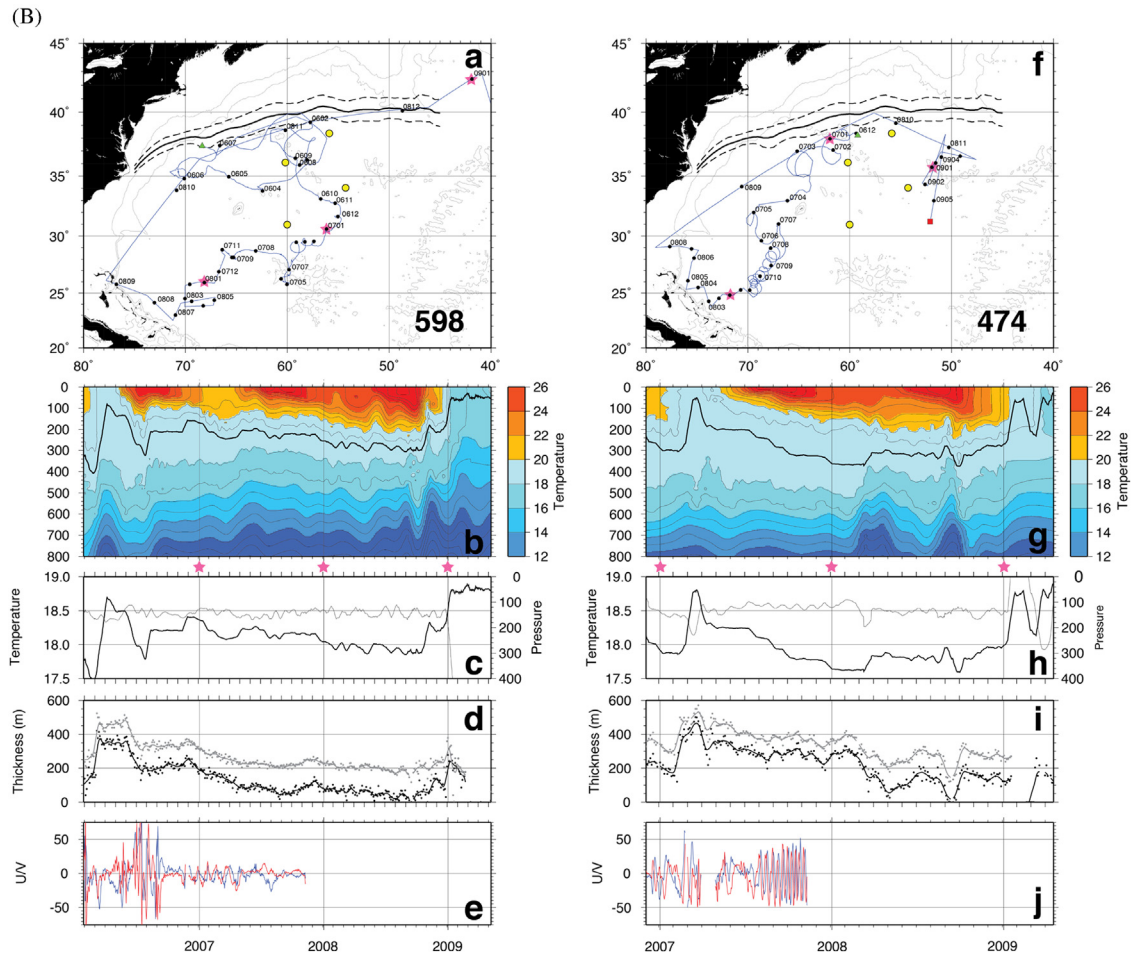


Fig. 13. Continued.

reported observations using 15-m drogued surface drifter data (Fratantoni, 2001). EKE values on the 18.5 °C isotherm are, as expected, substantially lower than surface values in the vicinity of the Gulf Stream. Both surface and subsurface fields exhibit a strong meridional gradient trending towards comparable, low EKE values in the gyre interior south of 33°N. Maximum EKE values observed at the EDW core depth are near  $1500 \text{ cm}^2/\text{s}^2$ . Recent work by Park et al. (2012) examines similarities between surface and subsurface eddy characteristics in this region.

Inhomogeneous deployment of drifting instruments in regions of strong eddy variability can introduce an array bias (Davis, 1991) on an estimate of the mean velocity field. For the substantially inhomogeneous bobber deployment strategy adopted during the CLIMODE field campaign we estimated the array bias associated with the mean velocity field shown in Fig. 17. Following Lavender et al. (2005), the array bias was computed as the product of a horizontal (isothermal) diffusivity parameter and the horizontal (isothermal) gradient of bobber concentration:  $u_{\text{array}} = -k \text{ grad}(\ln C)$ . The spatially-varying isothermal diffusivity  $k$  was estimated as the product of  $\langle u'v' \rangle$  (comparable to the EKE field shown in Fig. 18) and the integral timescale derived above (3 days). Bobber concentration  $C$  was approximated by the DOF field shown in Fig. 16b. The resulting vector velocity field describing the inherent array bias is shown in Fig. 19. Bias velocity magnitudes exceed 5 cm/s in close proximity to the Gulf Stream (where velocity variance and thus  $k$  is large) and along the edges of the sampled domain, especially in the far southwest corner. Overall, however, the magnitude of the array bias over the vast majority of the study region is small (less than 1 cm/s) and

does not fundamentally impact the interpretation of either Fig. 17 or those to follow.

#### 4.2. Spatial distribution of EDW

Temperature observations obtained by the CLIMODE bobbers were spatially and temporally averaged in a manner similar to the velocity observations described above. A  $2^\circ \times 2^\circ$  grid was used to generate record-length mean depictions of the depth of the 18.5 °C isotherm, the vertical thickness of the 17–19 °C layer, and the EDW column integral or “thickness” as defined in Appendix A. These results are shown in Fig. 20.

The mean topography of the 18.5 °C isotherm obtained from the bobber measurements (Fig. 20a) is quite similar to that derived from long-term climatology (Fig. 7) in both structure and magnitude. In particular, the mean 18.5 °C isotherm was found to be shallowest (50–100 m) in the northeast of the domain near 35°N, 50°W, and deepest (250–350 m) just south of the Gulf Stream and northeast of the Bahamas. These two relatively deep boundary regions are separated by a shallower zonal ridge extending westward along 32°N in both the bobber measurements and the climatology. This zonal ridge has similarities to the C-shaped surface dynamic height field shown by Reid (1978) inferred from hydrographic data, and to a weaker but similar feature in the satellite-derived absolute dynamic height field (Kwon and Riser, 2005; Rio et al., 2005). Note, however, that the C-shape quickly disappears in the subsurface dynamic heights, especially for the EDW layer (Kwon and Riser, 2004). The

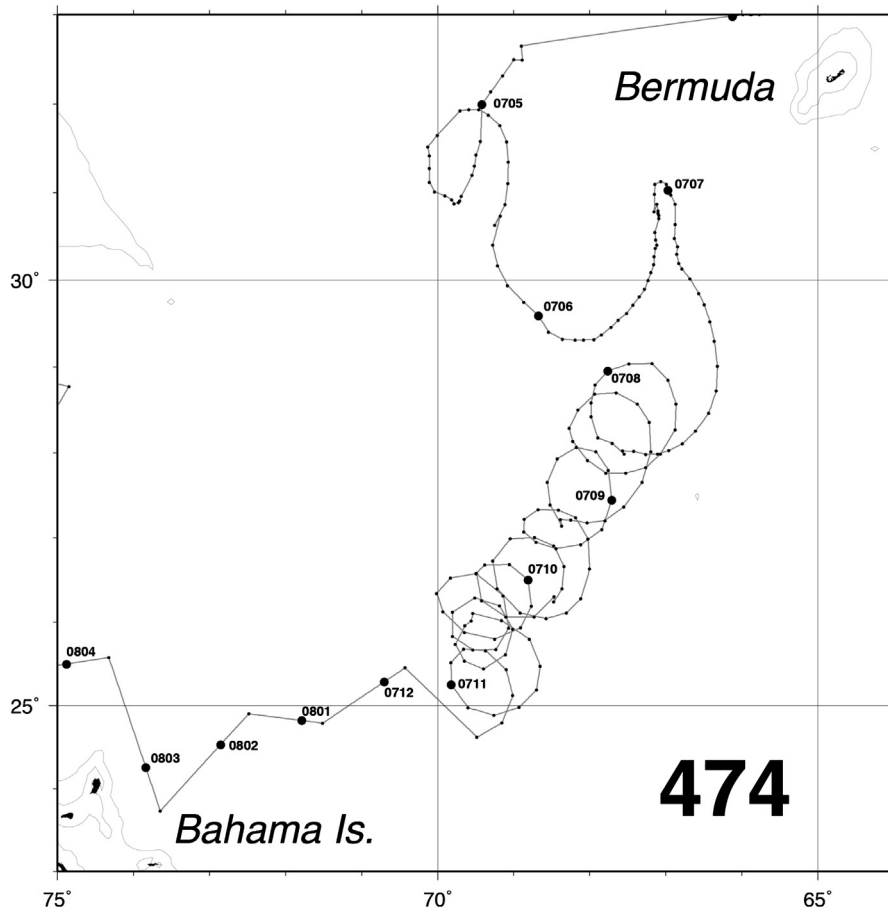


**Fig. 14.** Over 4 months bobber 474 was observed to complete at least 10 anticyclonic loops while translating southwestward towards the Bahamas. Recovery of the moored sound source array in November 2007 precluded direct observation of additional looping and the interaction between this eddy and the islands of the Bahamas. The observed loops were 40–50 km in radius with a 9–11-day rotational period. Maximum measured azimuthal velocity was approximately 55 cm/s. During this period the depth of the bobber increased slightly from 300 to 330 m while the local Eighteen Degree Water (EDW) thickness remained relatively constant near 300 m.

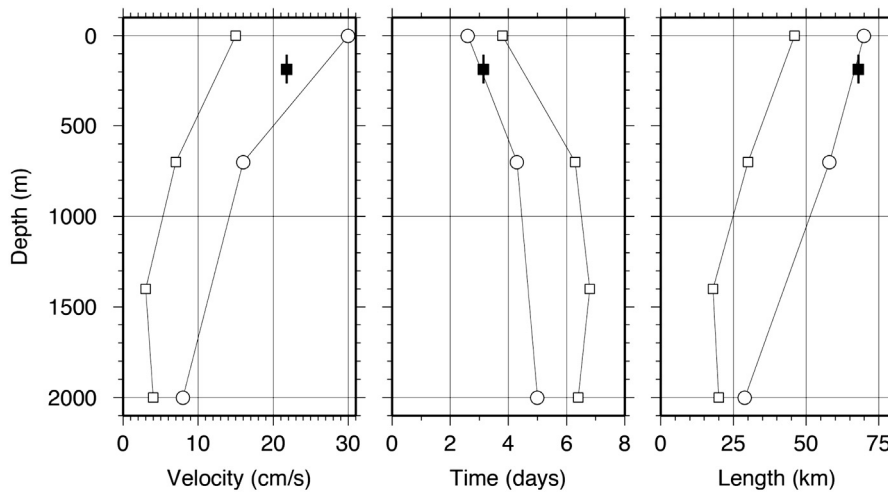


**Fig. 15.** Estimated Lagrangian velocity, time, and space scales derived from historical float and drifter measurements as originally reported by Lumpkin et al. (2002) compared with similar estimates from the CLIVAR Mode Water Dynamics Experiment (CLIMODE) bobbers. Values for each parameter are shown at several depths in the vicinity of the Gulf Stream extension (circles) and the southwestern subtropical gyre (squares). Parameters derived from a subset of the CLIMODE bobbers (squares; see text for details) are shown at the mean depth of valid RAFOS velocity measurements ( $185 \pm 80$  m). This figure adapted from Fig. 3 of Lumpkin et al. (2002). The originally published error bars and all measurements below 2000 m depth have been suppressed for clarity.

pronounced zonal gradient in isotherm depth near 57°W is coincident with enhanced southward flow as shown in Fig. 17.

Fig. 20b represents the record-length mean thickness of the vertical interval bounded by the 17 °C and 19 °C isotherms. When

compared to our best estimate of mean EDW thickness (Fig. 20c), which incorporates the temperature gradient criterion of Kwon and Riser (2004), several similarities and differences may be noted. First, the typical magnitude of the layer thickness differs

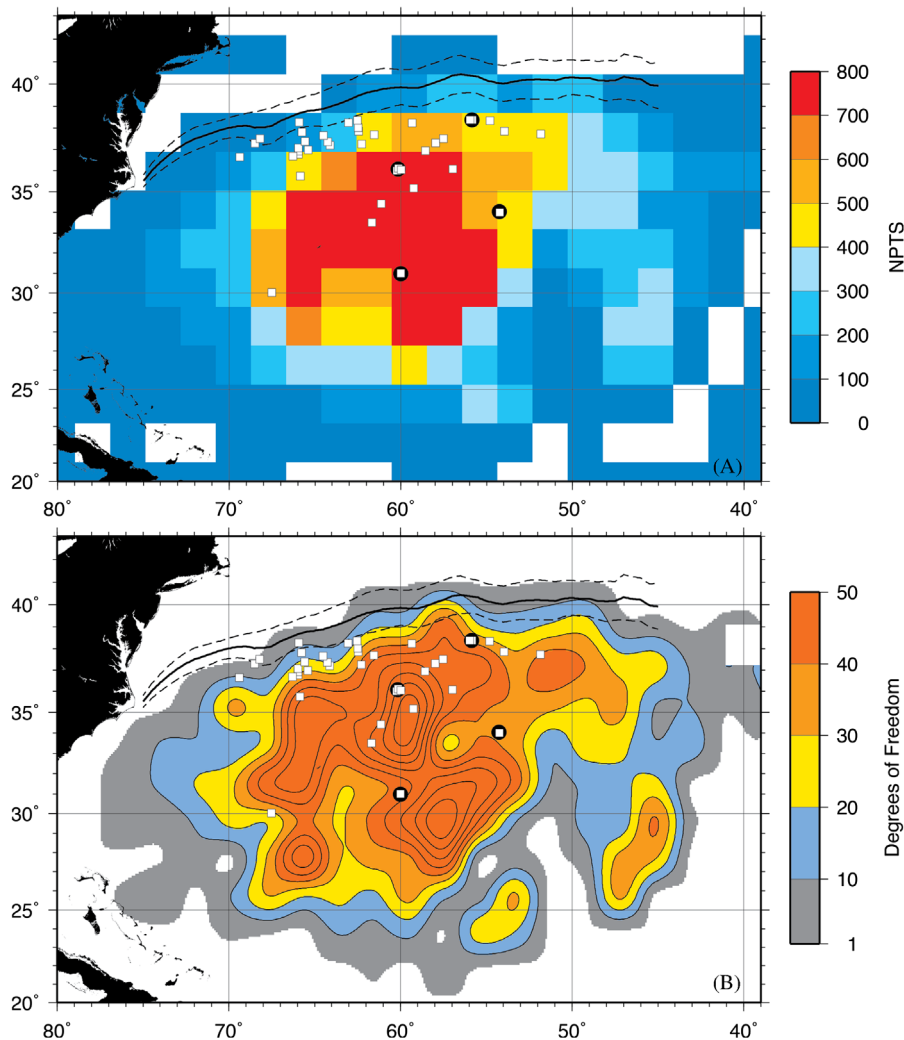


**Fig. 16.** (a) Raw count of RAFOS-derived velocity measurements per  $2^\circ$  square grid cell summed over the entire CLIVAR Mode Water Dynamics Experiment (CLIMODE) bobber record. (b) Contoured representation of the estimated number of degrees of freedom (DOF) per  $2^\circ$  grid cell for only those valid RAFOS-derived velocity measurements on the  $18.5^\circ\text{C}$  temperature surface. The contour interval is 10. Binned values obtained in regions with  $\text{DOF} < 10$  are not contoured and are suppressed in subsequent fields. Also shown in both panels are the initial deployment locations of the 40 CLIMODE bobbers (white squares).

by approximately 25%—the gradient criterion is substantially more restrictive. The general spatial patterns evident in both fields are comparable, with maximal thickness in the northeast of the domain and a zonal ridge along  $35^\circ\text{N}$ . Fig. 20c indicates that the region of thickest EDW is limited to a band extending approximately  $8\text{--}10^\circ$  south of the Gulf Stream axis and eastward to the mid-Atlantic Ridge—outside of this band EDW thickness vanishes rapidly. In contrast, the  $17\text{--}19^\circ\text{C}$  layer thickness remains non-zero well to the south and east of this band and, by construction, can never entirely vanish. Overall the thinning of EDW is noticeably greater in the western reaches of this zonal band when compared to the  $17\text{--}19^\circ\text{C}$  field. We interpret this as illustrating the progressive destruction of EDW with distance from the formation region.

While the bobber sampling is neither uniform nor extensive, the majority of the observed annual mean EDW volume is clearly isolated within a region bounded by the Gulf Stream, the mid-Atlantic Ridge, and  $25^\circ\text{N}$  latitude. The narrow extension of the thick EDW layer in the southwest corner of the domain is the result of a few bobbers looping within coherent vortices in this area (see below, Section 4.3). A strong lateral gradient in EDW thickness is evident extending southward from the Gulf Stream at

$45^\circ\text{W}\text{--}30^\circ\text{N}$ , and then westward along  $30^\circ\text{N}$ . Bobber trajectories (Fig. 12) and velocities (Fig. 17) indicate significant mean flow across this thickness gradient.

Away from the direct influence of the atmosphere the EDW thickness should decrease with time (and distance from the formation site) as vertical and horizontal mixing processes erode the layer's homogeneity (i.e. cause restratification). If wintertime atmospheric forcing along the southern edge of the Gulf Stream extension is the proximate cause for locally thick layers of EDW (e.g. Marshall et al., 2009) then Fig. 20 suggests that two segments of the Gulf Stream,  $65\text{--}75^\circ\text{W}$  and  $45\text{--}55^\circ\text{W}$ , may be important EDW source regions: local EDW thickness is greatest adjacent to the Gulf Stream in these areas. These two separate local maxima for the thickness of EDW (or the winter outcropping regions) are consistent with the previous observational studies (Joyce, 2012; Kwon and Riser, 2004; Talley and Raymer, 1982) as well as recent modeling studies (Douglass et al., 2013; Maze et al., 2013). In particular Joyce (2012) articulated that the western maximum is likely related to the non-advective EDW formation model of Warren (1972) and the eastern one is more consistent with the combination of the strong lateral advection and the air–sea cooling as described by Worthington (1959, 1976). In addition,

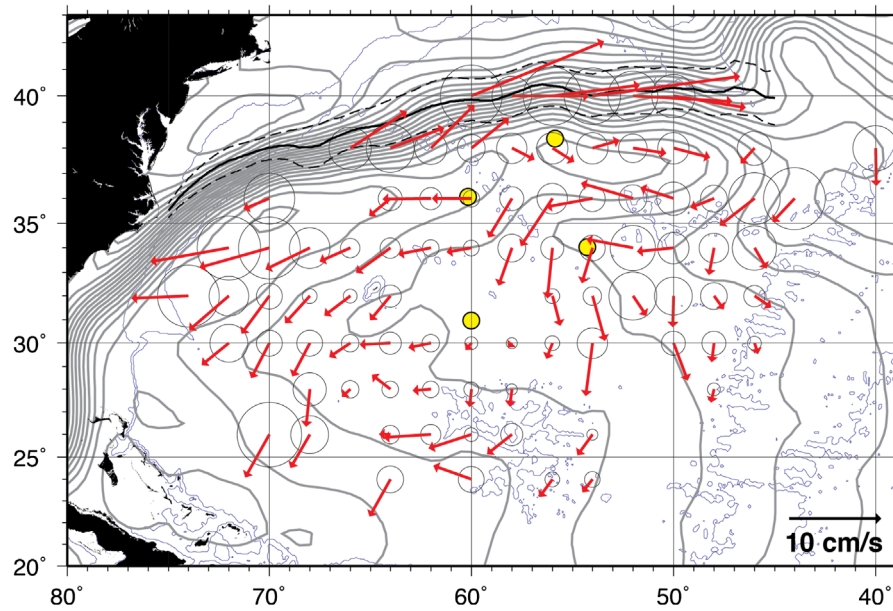


**Fig. 17.** Record-length mean vector velocity on the 18.5 °C temperature surface. Circles drawn at the root of each vector represent one standard error of the 2° binned velocity data. The velocity vector is suppressed in each grid cell with a mean velocity magnitude less than one standard error or with less than 10 degrees of freedom (DOF). Also shown (contours; interval=0.05 m) is the mean dynamic topography derived from satellite sea surface height measurements and the GRACE geoid (Jayne, 2006).

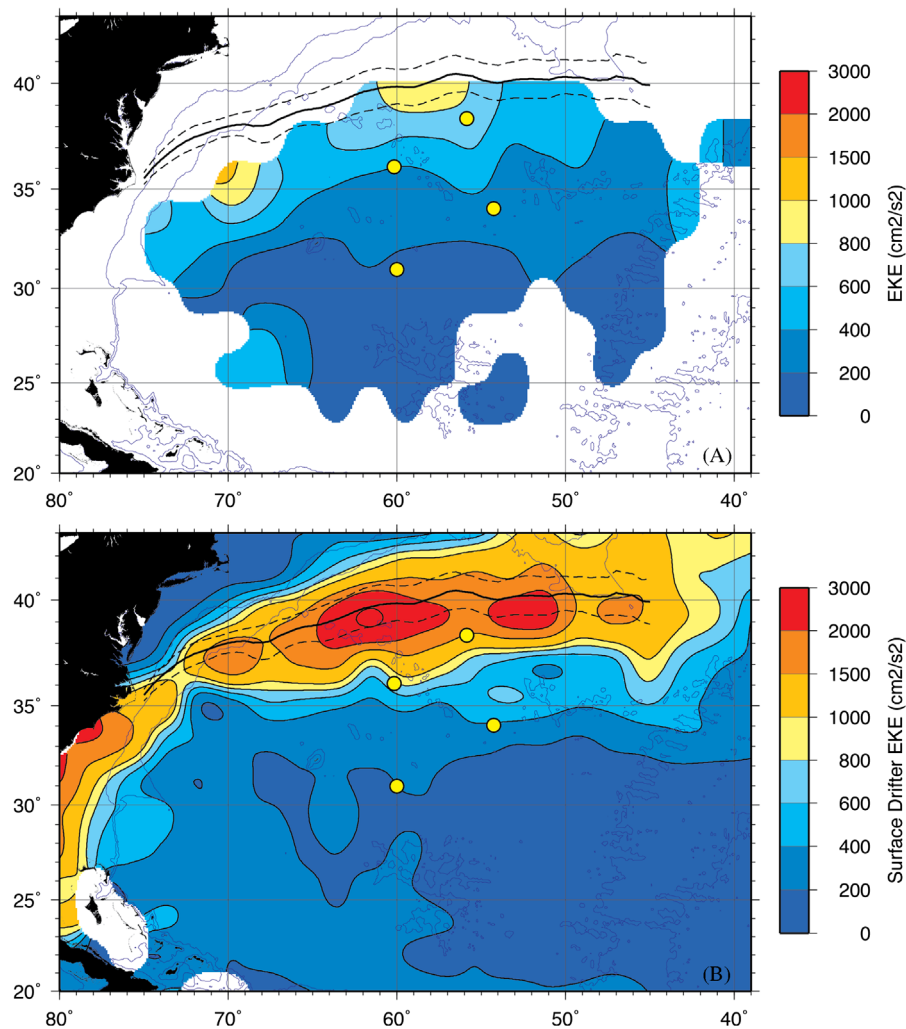


**Fig. 18.** (a) Record-length eddy kinetic energy (EKE) on the 18.5 °C temperature surface derived from CLIVAR Mode Water Dynamics Experiment (CLIMODE) bobber RAFOS velocity measurements. (b) Surface EKE derived from satellite-tracked surface drifter data as reported by Fratantoni (2001), remapped to a grid consistent with the subsurface bobber observations. Both fields have been spatially interpolated using a bi-cubic spline prior to contouring.

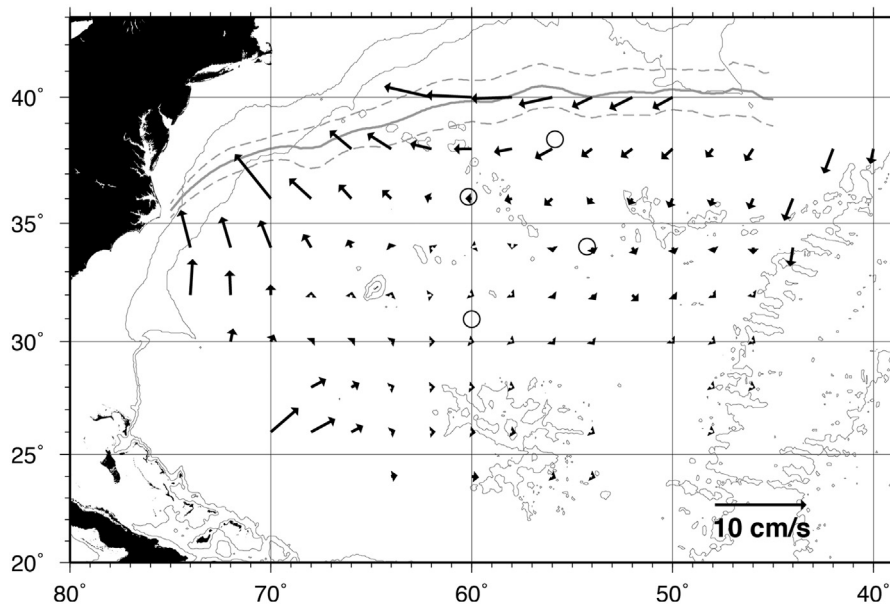


**Fig. 19.** The estimated array bias associated with the mean vector field shown in Fig. 17. The magnitude of the array bias over the core of our study region is less than 1 cm/s.

McGrath et al. (2010) reported that the two regions are separated by the minimum cross-frontal flow from the north across the Gulf Stream based on the surface drifter observations.

Seasonal subsets of the bobber temperature data were binned and mapped as above. Fig. 21 provides additional evidence of relatively localized EDW thickness maxima which we may interpret as either (a) regions of EDW formation, or (b) regions in which “old” EDW transported within the Gulf Stream is re-injected into the gyre interior. Note particularly the two segments of the wintertime Gulf Stream, identified in the paragraph above, adjacent to which lie substantial local maxima in EDW thickness extending southward into the gyre interior (Fig. 21e). Interestingly, Joyce et al. (2013) claim unusually large EDW production in a briefly-sampled region between 67 and 52°W—a region notable as a local minimum in EDW thickness in Fig. 21e. In contrast, the bobber-derived EDW thickness fields agree well with the inferred spatial pattern of EDW formation rate reported by Douglass et al. (2013), in a climatologically-forced numerical model. In that simulation there are two notable, isolated regions of EDW formation: a dominant region extending from 45 to 55°W, and a less vigorous region near 70°W.

Finally, it is interesting to note that the 17–19 °C and EDW layers exhibit seasonal layer thickness changes in the opposite sense: EDW thickness is generally greatest in winter, while the 17–19 °C layer is thickest in summer (see Fig. 21c–f). This is due to two fundamentally different forcing mechanisms: EDW layer thickness is dominated by buoyancy forcing during the winter formation period and gradually decreases during the rest of the year as EDW disperses and decays (Forget et al., 2011; Kwon and Riser, 2004). In contrast, the 17–19 °C layer thickness is maximal in summer due to seasonal wind forcing and Ekman pumping (see, e.g., Trenberth et al., 1990).

#### 4.3. EDW circulation

The two-dimensional fields presented above separately illustrate the mean circulation at the central depth of the EDW and the mean thickness of the EDW layer. In contrast, Fig. 22 was

constructed by bin-averaging (as above) daily values of the product of EDW thickness ( $h$ ) and RAFOS-derived velocity ( $u$ ) on the 18.5 °C isotherm. The resulting mean EDW thickness flux,  $\langle uh \rangle$ , field approximates the mean horizontal (isothermal) transport of EDW. The general pattern of EDW transport is similar to the velocity field shown in Fig. 17, with mean flow from the northeast to the southwest over much of the sampled region. This broad pattern is generally consistent with transport streamfunctions constructed by Kwon and Riser (2005) for the upper 900 m of the water column using Argo float hydrographic data.

Fig. 23 provides an integrated view of the record-length mean EDW thickness flux as a function of latitude and longitude. As can be inferred from the vector field in Fig. 22, southward transport of EDW is dominant at all latitudes within the sampled domain. In this annual representation, we observe nearly 20 Sv of EDW flowing southward across 32–34°N with substantial meridional divergence between 34 and 38°N. This region of divergence is consistent with the relatively thick zonal band of EDW along 35°N noted above. Westward transport increases from east to west reaching a maximum near 10 Sv at 70°W.

The depiction of a relatively narrow southward extension of the thick EDW layer in the southwest corner of the domain results almost entirely from a few bobbers (most notably 474; see Fig. 13b) which moved slowly through this area while looping within coherent vortices, and eventually experienced abrupt thinning of the EDW as the floats entered the strongly sheared western boundary current. The ability of submesoscale coherent vortices (e.g. McWilliams, 1985) to transport relatively undiluted ocean properties over substantial distances has been noted in several instances, most notably in the case of Mediterranean water eddies (Meddies; see Richardson et al., 2000, for a review). Meddies contribute substantially to the southwestward dispersal of saline water at mid-depth in the eastern Atlantic and have been suggested as comparable in importance to downgradient diffusion in maintaining the overall shape and intensity of the Mediterranean salt tongue (Wang and Dewar, 2003). While the relative importance of submesoscale coherent vortices in the dispersal of subducted EDW remains to be determined, it is clear from our limited observations that such features can have a profound effect on EDW distribution.

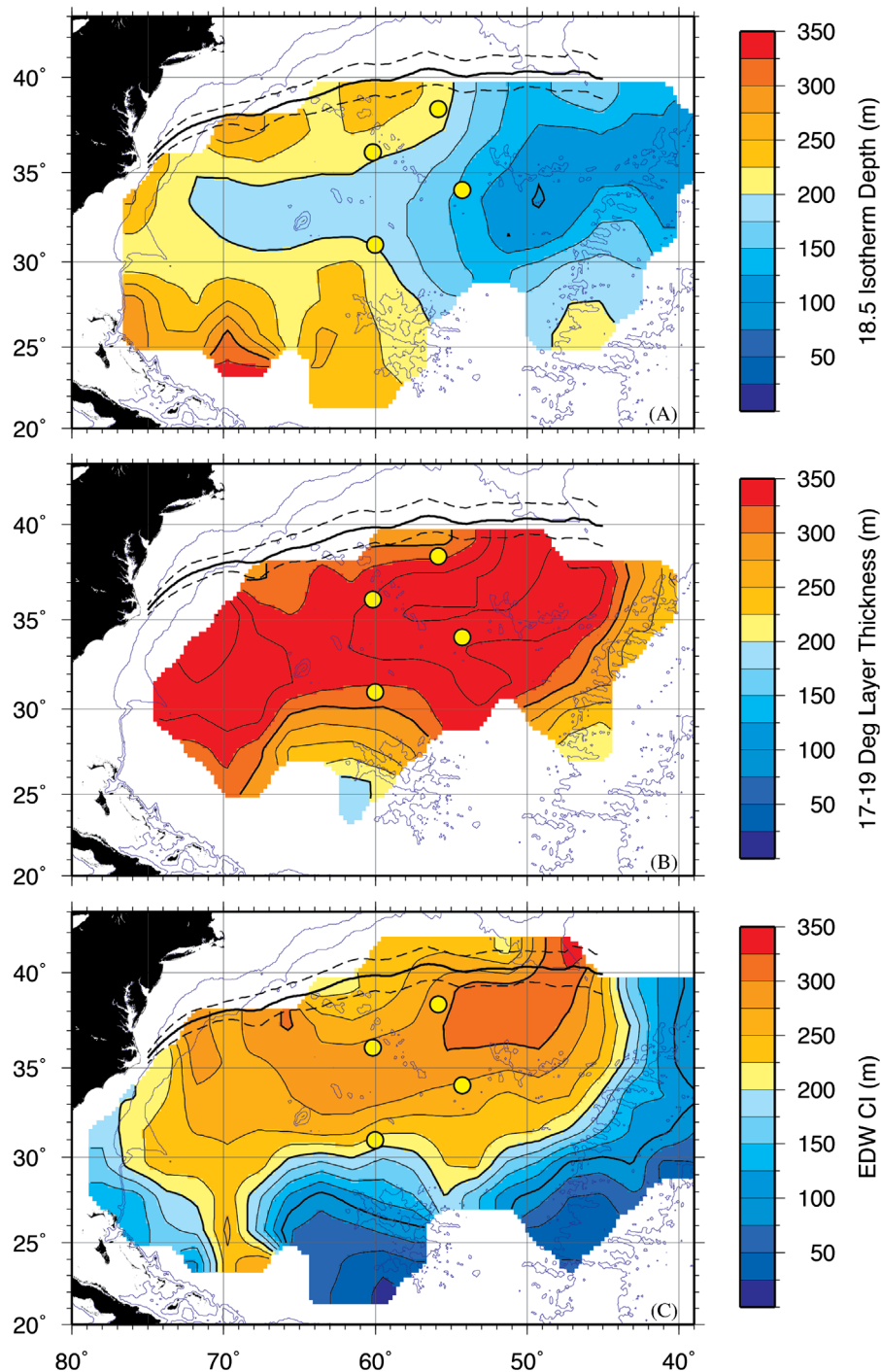


**Fig. 20.** Record-length mean fields of (a) 18.5 °C isotherm depth, (b) 17–19 °C layer thickness, and (c) Eighteen Degree Water (EDW) thickness (see Appendix A) derived from the CLIVAR Mode Water Dynamics Experiment (CLIMODE) bobber temperature profile measurements. Values were binned in  $2^\circ \times 2^\circ$  cells. No data are shown in grid cells with fewer than 10 independent measurements.

#### 4.4. EDW re-emergence and destruction

The CLIMODE bobbers spent all but approximately 12 hours of each 30-day period on their target isothermal surface. As such, they reasonably approximate the trajectory of an 18.5 °C parcel of water. As shown graphically in the case studies of Fig. 13A and B, the three-dimensional bobber trajectories collectively illustrate the subduction, translation, and eventual re-emergence of water parcels. We identified a total of 55 examples in which a bobber, initially in the mixed layer, was at some time later located beneath the stratified upper ocean, i.e. “subducted.” In this

analysis no distinction was made regarding the horizontal motion of the bobber: The assumed “subduction” could therefore occur via motion along a sloping isothermal surface into an area of persistent stratification, – or – via local restratification above a stationary bobber.

Fig. 24 presents a histogram summarizing these results. Shown is the interval between a bobber leaving and rejoining the surface mixed layer, with the requirement that these times are separated by a period of at least 6 months during which the bobber reported a stratified environment with surface temperature greater than 20 °C. Note that the number of examples exceeds the total

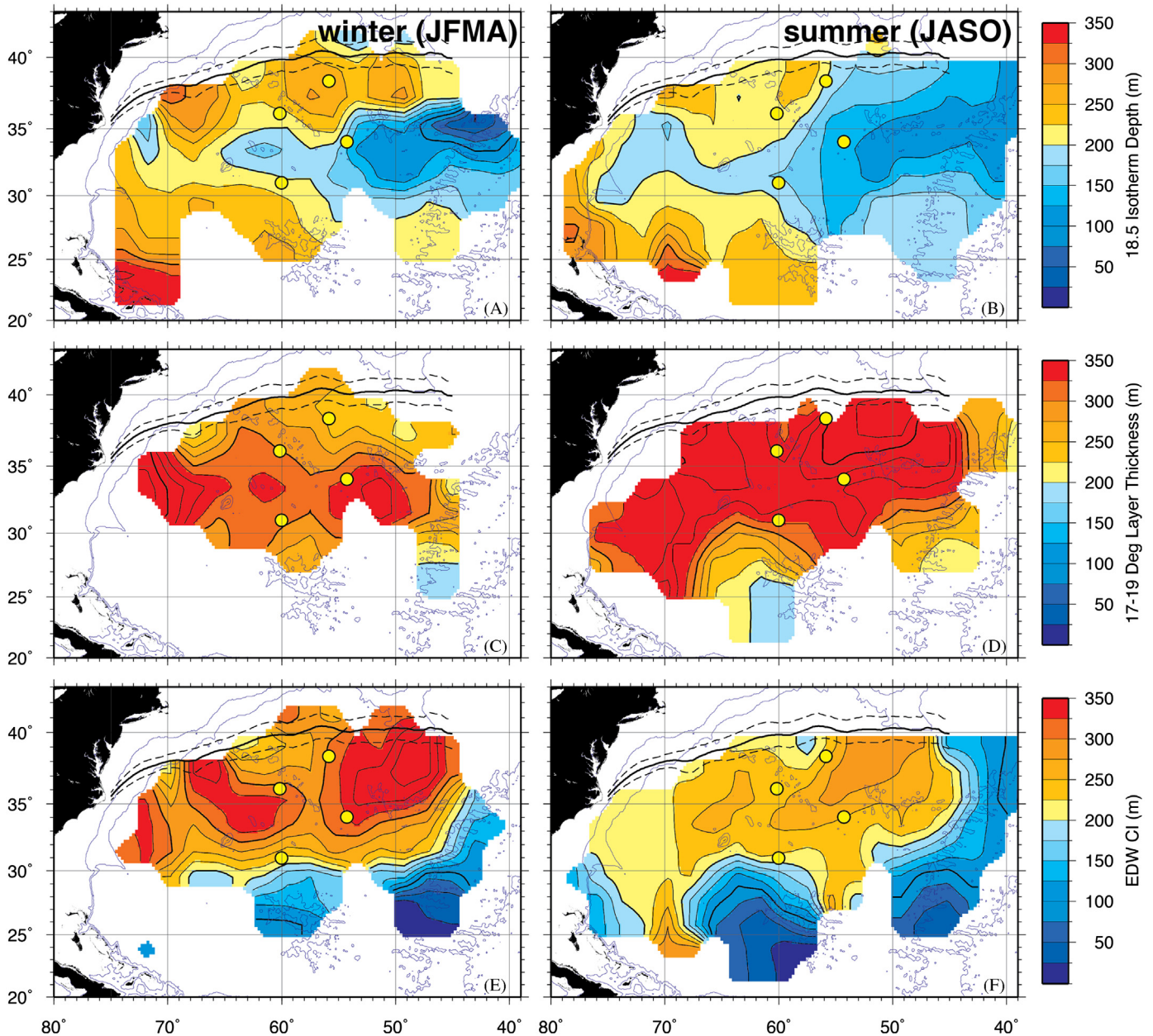


**Fig. 21.** As in Fig. 20, but seasonally averaged for boreal winter (left; January–April) and summer (right; July–October).

number of bobbers: those bobbers that recycled within the subtropical gyre (i.e. experienced more than one cycle of subduction and re-emergence) are included more than once in this tally.

There exists an inherent bias in this analysis due to the finite number of bobbers available, our targeted deployment strategy in the EDW formation region, and the limited time span of this experiment. However, our limited observations do clearly suggest that, contrary to previous hypotheses, subducted EDW is isolated from the atmosphere for only a short period of time. This is an unexpected result as previous data analysis efforts and modeling studies (e.g. Douglass et al., 2013; Forget et al., 2011; Kwon and Riser, 2004) have suggested EDW residence times of several years. One possible explanation for this discrepancy may be that mode water formed in different regions and/or different time periods is sequestered for varying durations. Such variance in the re-emergence timescale is supported by, for example, the modeling study of Douglass et al. (2013, see their Fig. 11) which reveals a highly skewed distribution of mode water ages with a peak near

2 years but an extended tail extending beyond 10 years. Given the temporally-limited span of our in situ observations (4 years) and their geographically non-uniform deployment, it is not surprising that we are unable to resolve such a distribution in full. However, the bobber observations clearly demonstrate that in the region of greatest EDW volume (i.e. Fig. 20c) in the northwestern subtropical gyre, short-term EDW sequestration (i.e. less than 24 months) is the more common scenario, and thus is the most relevant when considering climatic and biogeochemical consequences.

A careful analysis of the rates of EDW formation and destruction requires a well-resolved time series of basin-spanning EDW volume. Unfortunately, while spatial distribution of bobber-derived EDW thickness measurements is unusually dense for a short period of time, the aggregate observational density in both space and time is inadequate for a careful volumetric approach using the bobbers alone. Rather than applying extensive temporal and spatial interpolation to a sparse data set, we qualitatively examined all bobber-derived EDW thickness measurements to

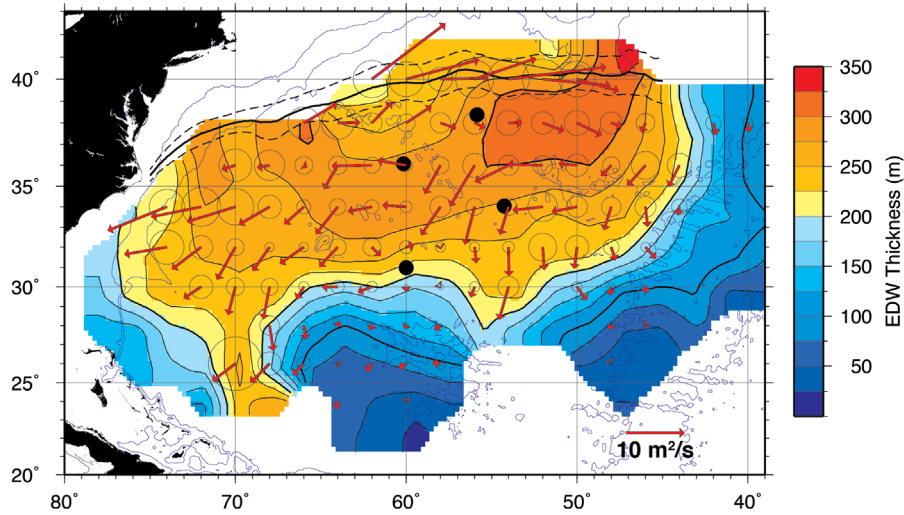


**Fig. 22.** Record-length mean Eighteen Degree Water (EDW) thickness flux,  $\langle uh \rangle$ , computed by bin-averaging daily values of the product of EDW thickness ( $h$ ) and RAFOS-derived velocity ( $\mathbf{u}$ ) on the 18.5 °C isotherm. The resulting field summarizes the mean horizontal (isothermal) transport of EDW in units of volume transport/width. Vectors with magnitude less than the bin-averaged standard error are suppressed for clarity.

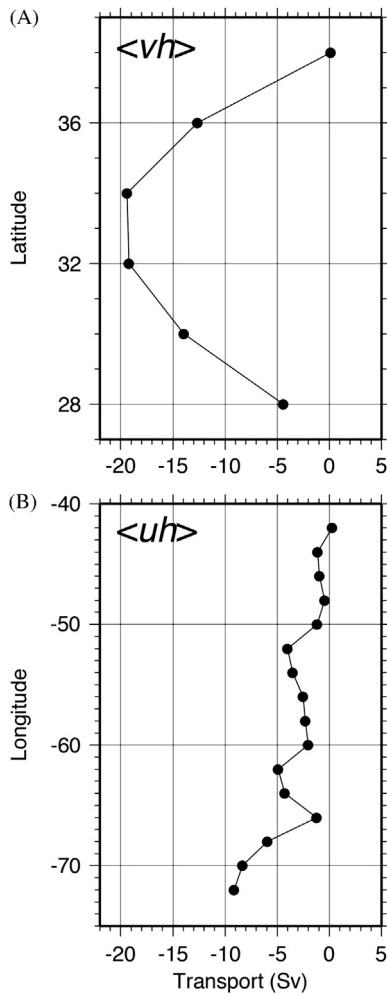


**Fig. 23.** Record-length mean transport of Eighteen Degree Water (EDW) as a function of (a) latitude (positive north) and (b) longitude (positive east) computed as per Fig. 22. Meridional transport was computed between 72 and 42°W. Zonal transport was computed between 28 and 38° N.

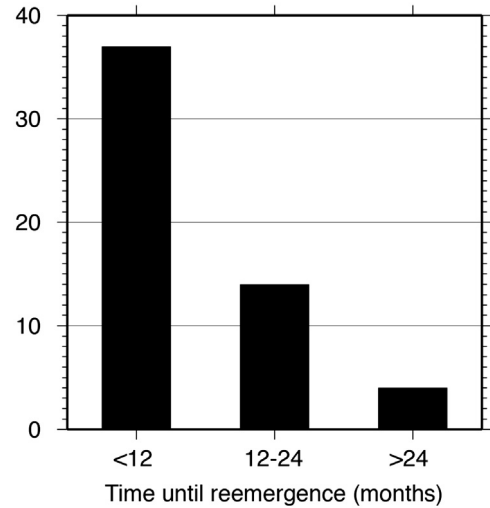


**Fig. 24.** Histogram summarizing the observed elapsed time between subduction and re-emergence of Eighteen Degree Water (EDW) as inferred from bobber measurements. A total of 55 examples were noted of a bobber, initially in the unstratified surface mixed layer, submerging beneath the seasonal stratification. In all but a very few cases, each of these bobbers was subsequently re-exposed to the mixed layer within 24 months. Note that the number of examples exceeds the number of bobbers: those bobbers that recycled within the subtropical gyre (i.e. experienced more than one cycle of subduction and re-emergence) are included more than once in this tally.

approximate the seasonality and rate of EDW thickness creation and destruction.

Fig. 25 illustrates a composite annual cycle of EDW thickness computed from all bobber temperature measurements during the CLIMODE field campaign. EDW thickness observations were binned using a 20 m vertical interval and a 10-day time period. The resulting 4-year average provides insight into the temporal variation of EDW thickness across the western subtropical Atlantic. In particular, we note that prior to late February there are extremely few observations of EDW layers with thickness greater than 300 m. In approximately the first week of March the number of thick EDW layers measurements increases dramatically. This

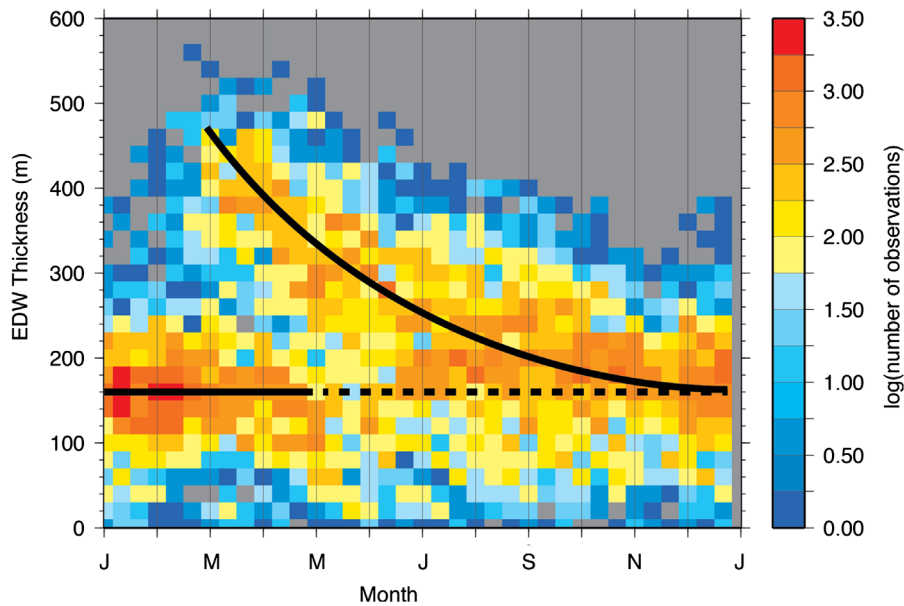


**Fig. 25.** Composite annual cycle of Eighteen Degree Water (EDW) thickness computed from all bobber temperature measurements during the CLIVAR Mode Water Dynamics Experiment (CLIMODE) field campaign. Colors represent the number of observations of EDW thickness in bins defined by a 20 m vertical interval and a 10-day period. The black lines were drawn subjectively to illustrate the annual evolution of EDW thickness in the western subtropical Atlantic.

general pattern is consistent with the volumetric analysis of Forget et al. (2011) derived from assimilating numerical model results, and with CLIMODE moored observations (Davis et al., 2013).

Also interesting is the bimodal distribution of EDW thickness between March and May. During this 3-month period there appears to be a distinction between “new” EDW (formed since late February) and “old” EDW. Approximately 6–9 months are required for the extremely thick “new” EDW layers to decay to background thickness levels. Based on the bobber-derived circulation and thickness maps we infer that much of this decay (i.e. restratification) occurs as mode water is transported southwestward in the subtropical gyre. It is apparent from the bobber trajectories that the western boundary (and the Gulf Stream) set an upper limit on the lifetime of a subducted EDW parcel.

## 5. Summary and conclusions

In this contribution we have presented initial results from a novel Lagrangian study of subtropical mode water stratification and circulation in the western North Atlantic. We illustrated the development and application of an array of acoustically-tracked, isotherm-following, bobbing profiling floats and described their application to a 4-year study of EDW dispersal and evolution.

The key results of this study may be summarized as follows:

1. The CLIMODE bobber program was an overwhelming technical success: 38 of 40 instruments achieved a success rate greater than 90%, and 37 of 40 were acoustically tracked for at least a portion of their lifetime (10–26 months). Operational endurance of the bobber array was substantially greater than anticipated with a half-life exceeding 4 years.
2. The bobber-derived Lagrangian integral time and length scales (3 days, 68 km) associated with motion on the 18.5 °C isothermal surface are consistent with previous measurements in the Gulf Stream extension region and fall between previous Lagrangian estimates at the ocean surface and thermocline depth. The first direct observations of circulation within the

EDW layer are indicative of substantial eddy activity both near the Gulf Stream and throughout the subtropical gyre. Evidence of long-lived submesoscale features associated with substantial EDW thickness suggests that coherent vortices may play an important role in the dispersal of mode water within the subtropical gyre.

3. We find that EDW (defined as a minimally-stratified layer) exhibits opposing seasonal thickness changes to a layer bounded simply by the 17–19 °C isotherms. EDW thickness is generally greatest in winter (as a result of buoyancy-forced convection), while the 17–19 °C layer is thickest in summer (resulting from Ekman pumping – vertical stretching – associated with basin-scale seasonal wind forcing.)
4. Finally, our limited observations suggest that, contrary to previous hypotheses, the majority of subducted EDW is isolated from the atmosphere for periods less than 24 months. Although our targeted deployment strategy imposed a spatial bias, and we were unable to directly observe longer-term EDW sequestration, seasonal-to-biennial re-emergence appears to be a common scenario which should be explored further and considered when assessing the climatic and biogeochemical consequences of EDW.

We anticipate further analyses of these data in the context of longer-term Argo float measurements, moored observations, and numerical modeling exercises. In particular, with our new understanding of the scope of the EDW pool in the subtropical western Atlantic it may be advantageous to explore numerical simulations with and without explicitly resolved submesoscale eddies. In addition to facilitating the widespread dispersal of EDW, such translating eddies may also contribute to the large variance in EDW age/re-emergence time by transporting and isolating mode water away from the dissipative western boundary.

## Acknowledgments

The authors acknowledge the logistical and scientific cooperation of our CLIMODE collaborators, the technical support of Mr. John Lund, and the able assistance of the captains and crew of the

WHOI research vessels *Oceanus*, *Knorr*, and *Atlantis*. Ellyn Montgomery, Terry McKee, and Heather Furey contributed significantly to the development of software and methods for bobber tracking and data processing. We thank Fiamma Straneo (WHOI) and Bernadette Sloyan (CSIRO) for substantial contributions to the planning of this field experiment. We acknowledge the careful work of three anonymous reviewers whose thoughtful comments and suggestions greatly improved this manuscript. This work was supported by the U.S. National Science Foundation under Grant nos. OCE-0424492 and OCE-0961090.

## Appendix A. EDW thickness estimation

Temporal and spatial variations over the expanse of the western Atlantic make it challenging to uniquely define EDW based on measured water properties (e.g. Joyce, 2012). Worthington (1959) defined EDW in terms of a specific temperature and salinity range ( $17.9\text{ }^{\circ}\text{C} \pm 0.3\text{ }^{\circ}\text{C}$ ;  $36.5 \pm 0.1$ ). More recent work by Klein and Hogg (1996), Alfultis and Cornillon (2001), and Kwon and Riser (2004) have explicitly incorporated the vertically-homogenous nature of the EDW layer by including in their analyses potential vorticity and/or vertical temperature gradient criteria. These latter definitions are somewhat more flexible because, as noted by Talley and Raymer (1982) and Klein and Hogg (1996), the specific temperature–salinity (T–S) characteristics of EDW may vary interannually.

In this contribution we adopt the Kwon and Riser (2004) EDW definition based on temperature and temperature gradient. Peng et al. (2006) used Argo float profiles to explore the sensitivity of EDW volume estimates to variations in the choice of temperature gradient threshold. They found that a slightly relaxed vertical temperature gradient criterion vs. that used by Kwon and Riser (2004) ( $0.01\text{ }^{\circ}\text{C}/\text{m}$  vs.  $0.006\text{ }^{\circ}\text{C}/\text{m}$ ) resulted in a factor-of-two increase in inferred EDW volume. For ease in comparison with previous observational results we apply here the original Kwon and Riser (2004) criteria. Specifically, we label a particular vertical segment of a temperature profile as EDW if (a) the temperature falls between 17 and 19  $^{\circ}\text{C}$  and (b) the local vertical temperature gradient is less than  $0.006\text{ }^{\circ}\text{C}/\text{m}$ .

A complication that arises from the use of fixed criteria as above is the possibility of identifying multiple, inconsequentially-different, layers separated by regions of slightly different temperatures or temperature gradients (see e.g. Fig. 1). While such multi-layered structures may be both real and relevant, for this basin-scale overview we integrate the total EDW contribution of such layers using the following procedure: each temperature profile (with nominal 5–20 m resolution) is vertically interpolated using a shape-preserving cubic spline to a uniform 1 m interval. The vertical temperature gradient is computed from the interpolated profile. We define the local EDW thickness (or more precisely, the column integral of water with EDW characteristics) as the sum of all 1 m bins in the profile meeting both the temperature range and temperature gradient criteria described above. This method is simple, objective, provides thickness estimates that are robust to small variations in both temperature and temperature gradient about the threshold criteria, and yields a conservative lower bound on the actual EDW thickness and volume using the Kwon and Riser (2004) definition.

## References

- Alfultis, M.A., Cornillon, P., 2001. Annual and interannual changes in the North Atlantic STMW layer properties. *J. Phys. Oceanogr.* 31, 2066–2086.
- Bates, N.R., Pequignot, A.C., Johnson, R.J., Gruber, N., 2002. A short-term sink for atmospheric  $\text{CO}_2$  in subtropical mode water of the North Atlantic Ocean. *Nature* 420, 489–493.
- Brambilla, E., Talley, L.D., 2006. Surface drifter exchange between the North Atlantic subtropical and subpolar gyres. *J. Geophys. Res.* 111 (C07026), 16, <http://dx.doi.org/10.1029/2005JC003146>.
- Chelton, D.B., de Szoeke, R.A., Schlax, M.G., El Naggar, K., Siwertz, N., 1998. Geographical variability of the first baroclinic Rossby radius of deformation. *J. Phys. Oceanogr.* 28, 433–460.
- Curry, R.G., 1996. Hydrobase—A Database of Hydrographic Stations and Tools for Climatological Analysis. Woods Hole Oceanographic Institution Technical Report WHOI-96-01, 44 pp.
- Davis, R.E., 1991. Observing the general circulation with floats. *Deep-Sea Res.* 38 (1), S531–S571.
- Davis, R.E., Sherman, J.T., Dufour, J., 2001. Profiling ALACEs and other advances in autonomous subsurface floats. *J. Atmos. Ocean. Tech.* 18, 982–993.
- Davis, R.E., Webb, D.C., Regier, L.A., Dufour, J., 1992. The autonomous Lagrangian circulation explorer (ALACE). *J. Atm. Oceanic Tech.* 9, 264–285.
- Davis, X.J., Straneo, F., Kwon, Y.-O., Kelly, K.A., Toole, J.M., 2013. Evolution and formation of North Atlantic Eighteen Degree Water in the Sargasso Sea from Moored data. *Deep-Sea Res. II* 91, 11–24.
- Dong, S., Gille, S.T., Sprintall, J., 2007. An assessment of the Southern Ocean mixed layer heat budget. *J. Climate* 20, 4425–4442.
- Dong, S., Kelly, K.A., 2004. Heat budget in the Gulf Stream region: the importance of heat storage and advection. *J. Phys. Oceanogr.* 34, 1214–1231.
- Douglass, E.M., Kwon, Y.-O., Jayne, S.R., 2013. A comparison of North Pacific and North Atlantic subtropical mode waters in a climatologically-forced model. *Deep-Sea Res. II* 91, 139–151.
- Forget, G., Maze, G., Buckley, M., Marshall, J., 2011. Estimated seasonal cycle of North Atlantic Eighteen Degree Water volume. *J. Phys. Oceanogr.* 41 (2), 269–286.
- Fratantoni, D.M., 2001. North Atlantic surface circulation during the 1990's observed with satellite-tracked drifters. *J. Geophys. Res.* 106 (C10), 22,067–22,093.
- Fratantoni, D.M., T.K. McKee, B.A. Hodges, H.H. Furey, J.M. Lund, 2010. CLIMODE Bobber Data Report: July 2005–May 2009. Woods Hole Oceanographic Institution Technical Report WHOI-2010-03, 154 pp.
- Hanawa, K., Talley, L.D., 2001. Mode waters. Ocean circulation and climate. In: Siedler, J., Church, J. (Eds.), *International Geophysics Series*. Academic Press, pp. 373–386.
- Jayne, S.R., 2006. Circulation of the North Atlantic Ocean from altimetry and the gravity recovery and climate experiment geoid. *J. Geophys. Res.*, 111, <http://dx.doi.org/10.1029/2005JC003128>.
- Joyce, T.M., 2012. New perspectives on eighteen-degree water formation in the North Atlantic. *J. Oceanogr.* 68 (1), 45–52, <http://dx.doi.org/10.1007/s10872-011-0029-0>.
- Joyce, T.M., Kwon, Y.-O., Yu, L., 2009. On the relationship between synoptic wintertime atmospheric variability and path shifts in the Gulf Stream and the Kuroshio extension. *J. Climate* 22 (12), 3177–3192.
- Joyce, T.M., Luyten, J.R., Kubryakov, A., Bahr, F.B., Pallant, J.S., 1998. Meso- to large-scale structure of subducting water in the subtropical gyre of the eastern North Atlantic Ocean. *J. Phys. Oceanogr.* 28 (1), 4061.
- Joyce, T.M., Thomas, L.N., Dewar, W.K., Girtton, J.B., 2013. Eighteen Degree Water formation within the Gulf Stream: a new paradigm arising from CLIMODE. *Deep-Sea Res. II* 91, 1–10.
- Klein, B., Hogg, N., 1996. On the variability of 18 Degree Water formation as observed from moored instruments at 55° W. *Deep-Sea Res.* 43 (1112), 1777–1806.
- Kwon, Y.-O., 2003. Observation of general circulation and water mass variability in the North Atlantic subtropical mode water region. Ph.D. thesis, University of Washington, 161 pp.
- Kwon, Y.-O., Riser, S.C., 2004. North Atlantic Subtropical Mode Water: A history of ocean-atmosphere interaction 1961–2000. *Geophys. Res. Lett.* 31, L19307, <http://dx.doi.org/10.1029/2004GL021116>.
- Kwon, Y.-O., Riser, S.C., 2005. General circulation of the western subtropical North Atlantic observed using profiling floats. *J. Geophys. Res.* 110, C10012, <http://dx.doi.org/10.1029/2005JC002909>.
- Laine, E.P., Hollister, C.D., 1981. Geological effects of the Gulf Stream system on the northern Bermuda Rise. *Marine Geology* 39, 277–310.
- Lavender, K.L., Owens, W.B., Davis, R.E., 2005. The mid-depth circulation of the subpolar North Atlantic Ocean as measured by subsurface floats. *Deep-Sea Res.* 52, 767–785.
- Lumpkin, R., Tréguier, A.-M., Speer, K., 2002. Lagrangian Eddy scales in the North Atlantic Ocean. *J. Phys. Oceanogr.* 32, 2425–2440.
- Lund, S.P., Keigwin, L., 1994. Measurement of the degree of smoothing in sediment paleomagnetic secular variation records: an example from late Quaternary deep-sea sediments of the Bermuda Rise, western north Atlantic Ocean. *Earth Planet. Sci. Lett.* 122, 317–330.
- Marshall, J., Andersson, A., Bates, N., Dewar, W., Doney, S., Edson, J., Ferrari, R., Forget, G., Fratantoni, D., Gregg, M., Joyce, T., Kelly, K., Lozier, S., Lumpkin, R., Maze, G., Palter, J., Samelson, R., Silverthorne, K., Skillingstad, E., Straneo, F., Talley, L., Thomas, L., Toole, J., Weller, R., 2009. The climate field campaign: observing the cycle of convection and restratification over the Gulf Stream. *Bull. Am. Meteor. Soc.* 90, 1337–1350.
- Maze, G., Deshayes, J., Marshall, J., Tréguier, A.-M., Chronis, A., Vollmer, L., 2013. Surface vertical PV fluxes and subtropical mode water formation in an eddy-resolving numerical simulation. *Deep-Sea Res. II* 91, 128–138.
- McGrath, G.G., Rossby, T., Merrill, J.T., 2010. Drifters in the Gulf Stream. *J. Mar. Res.* 68, 699–721.

- McWilliams, J.C., 1985. Submesoscale, coherent vortices in the ocean. *Rev. Geophys.* 23, 165–182.
- Old, E., Haines, K., 2006. North Atlantic subtropical mode waters and ocean memory in HadCM3. *J. Climate* 19, 1126–1148.
- Palter, J.B., Lozier, M.S., Barber, R.T., 2005. The effect of advection on the nutrient reservoir in the North Atlantic subtropical gyre. *Nature* 437, 687–692.
- Park, J.J., D.M. Fratantoni, Y.-O. Kwon, M.S. Lozier, 2012. Patchiness Length Scale of Eighteen Degree Water. Poster Presentation at AGU Ocean Sciences Meeting, Salt Lake City, UT.
- Peng, G., Chassignet, E.P., Kwon, Y.-O., Riser, S.C., 2006. Investigation of the variability of the North Atlantic subtropical mode water using profile float data and numerical model output. *Ocean Model.* 13, 65–85.
- Reid, J., 1978. On the middepth circulation and salinity field in the North Atlantic Ocean. *J. Geophys. Res.* 83 (10), 5063, <http://dx.doi.org/10.1029/JC083iC10p05063>.
- Richardson, P.L., Bower, A., Zenk, W., 2000. A census of meddies tracked by floats. *Prog. Oceanogr.* 45, 209–250, Pergamon.
- Rio, M.-H., P. Schaeffer, J.-M. Lemoine, F. Hernandez, 2005. Estimation of the ocean mean dynamic topography through the combination of altimetric data, in situ measurements and GRACE geoid: from global to regional studies. In: Proceedings of the GOCINA international workshop, Luxembourg.
- Roemmich, D., Belbeoch, M., Freeland, H., Garzoli, S.L., Gould, W.J., Grant, F., Ignaszewski, M., King, B., Klein, B., Le Traon, P.-Y., Mork, K.A., Owens, W.B., Pouliquen, S., Ravichandran, M., Riser, S., Sterl, A., Suga, T., Suk, M.-S., Sutton, P., Thierry, V., Velez-Belchi, P.J., Wijffels, S., Xu, J., 2009. Argo: the challenge of continuing 10 years of progress. *Oceanography* 22 (3), 46–55.
- Rosby, T., Dorson, D., Fontaine, J., 1986. The RAFOS system. *J. Atmos. Ocean. Technol.* 3, 672–679 [http://www.dx.doi.org/10.1175/1520-0426\(1986\)003%3c0672:TRS%3e2.0.CO;2](http://www.dx.doi.org/10.1175/1520-0426(1986)003%3c0672:TRS%3e2.0.CO;2).
- Rosby, T., Prater, M.D., 2005. On variations in static stability along Lagrangian trajectories. *Deep-Sea Res. II* 52 (3–4), 465–479, <http://dx.doi.org/10.1016/j.dsr2.2004.12.003>.
- Rosby, H.T., Riser, S.C., Mariano, A.J., 1983. The western north Atlantic—a Lagrangian view point. In: Robinson, A.R. (Ed.), *Eddies Marine science*. Springer-Verlag, Berlin, pp. 66–91.
- Rosby, H.T., Voorhis, A.D., Webb, D., 1975. A Quasi-Lagrangian study of mid-ocean variability using long range SOFAR floats. *J. Mar. Res.* 33, 355–382.
- Rypina, I.I., Pratt, L.J., Lozier, M.S., 2011. Near-surface transport pathways in the North Atlantic Ocean: looking for throughput from the subtropical to the Subpolar Gyre. *J. Phys. Oceanogr.* 41, 911–925.
- Siegel, D.A., Doney, S.C., Yoder, J.A., 2002. The North Atlantic spring phytoplankton bloom and Sverdrup's critical depth hypothesis. *Science* 296 (5568), 730–733, <http://dx.doi.org/10.1126/science.1069174>.
- Speer, K., Tziperman, E., 1992. Rates of water mass formation in the North Atlantic Ocean. *J. Phys. Oceanogr.* 22, 93–104.
- Talley, L.D., Raymer, M.E., 1982. Eighteen Degree Water variability. *J. Mar. Res.* 40, 757–777, Suppl.
- Thomas, L.N., 2005. Destruction of potential vorticity by winds. *J. Phys. Oceanogr.* 35, 2457–2466.
- Thomas, L.N., Joyce, T.M., 2010. Subduction on the northern and southern flanks of the Gulf Stream. *J. Phys. Oceanogr.* 40, 429–438.
- Trenberth, K.E., Large, W.G., Olson, J.G., 1990. The mean annual cycle in global ocean wind stress. *J. Phys. Oceanogr.* 20, 1742–1760.
- Wang, G., Dewar, W.K., 2003. Meddy–Seamount interactions: implications for the Mediterranean Salt Tongue. *J. Phys. Oceanogr.* 33, 2446–2461.
- Warren, B.A., 1972. In sensitivity of subtropical mode water characteristics to meteorological fluctuations. *Deep-Sea Res.* 19, 1–19.
- Wooding, C.M., H.H. Furey, M.A. Pacheco, 2005. RAFOS Float Processing at the Woods Hole Oceanographic Institution. Woods Hole Oceanographic Institution Technical Report WHOI-2005-02, 37 pp.
- Worthington, L.V., 1959. The 18° water in the Sargasso Sea. *Deep-Sea Res.* 5, 297–305.
- Worthington, L.V., 1972. Negative oceanic heat flux as a cause of water-mass formation. *J. Phys. Oceanogr.* 2 (3), 205–211.
- Worthington, L.V., 1976. On the North Atlantic circulation. *The Johns Hopkins Oceanogr. Stud.* 6. The John Hopkins Press 110 pp.